CLIMATE CHANGE, INEQUALITY, AND HUMAN MIGRATION

Michał Burzyński
Luxembourg Institute of Socio-Economic Research (LISER), Luxembourg

Christoph Deuster
Institute for Employment Research (IAB), Germany

Frédéric Docquier
Luxembourg Institute of Socio-Economic Research (LISER), Luxembourg
Department of Economics and Management, University of Luxembourg, Luxembourg

Jaime de Melo
Université de Genève, Switzerland and Fondation pour les études et recherches sur le développement international (FERDI)

Abstract
This paper investigates the long-term implications of climate change on global migration and inequality. Accounting for the effects of changing temperatures, sea levels, and the frequency and intensity of natural disasters, we model the impact of climate change on productivity and utility in a dynamic general equilibrium framework. By endogenizing people's migration decisions across millions of 5×5 km spatial cells, our approach sheds light on the magnitude and dyadic, education-specific structure of human migration induced by global warming. We find that climate change strongly intensifies global inequality and poverty, reinforces urbanization, and boosts migration from low- to high-latitude areas. Median projections suggest that climate change will induce a voluntary and a forced permanent relocation of 62 million working-age individuals over the course of the 21st century. Overall, under current international migration laws and policies, only a small fraction of people suffering from the negative effects of climate change manages to move beyond their homelands. We conclude that it is unlikely that climate shocks will induce massive international flows

The editor in charge of this paper was Giovanni Peri.

Acknowledgments: We thank the editor and five anonymous referees for their comments and suggestions. This paper benefitted from helpful remarks from Catia Batista, Michel Beine, Simone Bertoli, Carlo Carraro, Klaus Desmet, François Gemenne, Fabio Mariani, Katrin Millock, Lionel Ragot, Hillel Rapoport, and Pedro Vicente. We acknowledge financial support from the *Agence Française de Développement* (convention IRS/ECO/437-2017). Frédéric Docquier acknowledges financial support from the ARC convention on "New approaches to understanding and modelling global migration trends" (convention 18/23-091). Jaime de Melo acknowledges support from the French National Research Agency under program ANR-10-LABX-14-01.

E-mail: michal.burzynski@liser.lu (Burzyński); christoph.deuster@iab.de (Deuster); frederic.docquier@liser.lu (Docquier); jaime.demelo@unige.ch (de Melo)

Journal of the European Economic Association 2022 20(3):1145–1197
https://doi.org/10.1093/jeea/jvab054

of migrants, except under combined extremely pessimistic climate scenarios and highly permissive migration policies. In contrast, poverty resulting from climate change is a real threat to all of us. (JEL: F22, E24, Q54, J61, O15)

Teaching Slides
A set of Teaching Slides to accompany this article are available online as Supplementary Data.

1. Introduction

Climate change (CC) is one of the biggest threats that humankind has ever faced in modern history (IPCC 2014, 2021). Anthropogenic emissions of carbon dioxide have begun to induce changes in global climatic conditions and local environments in most regions of the world. Almost certainly, these changes will intensify in the coming decades.[1] Abundant climatological research finds that CC not only results in hotter temperatures and higher ocean levels (Stocker et al. 2013), but is also responsible for the increased frequency and intensity of extreme weather events and natural disasters (Stott 2016). CC is likely to adversely impact people's well-being through multiple channels, such as labor productivity, working and living conditions, food security, access to water and natural resources, consumption of electricity, health outcomes, destruction of assets, crime, political tensions, and instability (Dell, Jones, and Olken 2014; Carleton and Hsiang 2016).

Crucially, the consequences of economic and social damage caused by CC are likely to vary over time and space. First, the economic effects of temperature changes will differ across sectors and latitudes, as the relationship between temperature and productivity is sector-specific and nonlinear (i.e. the effects are dependent on current levels of temperature). Low-latitude countries in general, and their rural regions in particular, have contributed the least to CC, but these areas will be the most adversely affected. Second, coastal areas are heterogeneously exposed to rising sea levels, which depends not only on the projected ocean levels, but also on the population distribution by elevation in the regions at risk. Third, responses to global warming are likely to vary with local topographical, hydrological, and ecological characteristics, thus exogenously predetermining the livability of a given area. Fourth, countries differ in their ability to provide efficient mitigation strategies against flooding. The most tragic consequences of coastal flooding and natural disasters occur in poor nations, where

1. According to IPCC (2021), in 2010–2020, increases in the global mean surface temperature and the sea level equal, respectively, 1.1°C (2.0°F) and 0.2 m since the pre-industrial period (1850–1900). Evidence shows that these increases have accelerated since 1980 (IPCC 2021). Climatologists estimate that average global temperatures might further increase by 2.5°C–4.0°C (4.5°F–7.2°F) over the current century. Recent studies suggest that, after allowing for incremental changes from storm surges, the global sea level could rise by 1–2 m before the end of the century (e.g. Rigaud et al. 2018).

the infrastructure to protect people and respond to shocks is lacking. These countries remain the most vulnerable to potential future losses as their exposition to extreme weather events is projected to increase drastically.

By imposing heterogeneous damage across countries, regions, and localities—including very specific areas that are bound to become partly or totally inhabitable—CC will increase voluntary human migration and forced displacement over the course of the 21st century. Responses to CC will depend on local socio-economic factors, such as individual capacity and willingness to migrate, social cohesion and networks, and the engagement of political authorities. As global warming projections become increasingly alarming, the questions of (i) how many people will migrate, (ii) the characteristics of these migrants, (iii) where they come from and where they go, and (iv) the socio-economic implications of climate migration have become a source of controversy in the literature (Boas et al. 2019; McLeman 2019; Conte et al. 2021), gaining unprecedented attention in public discourse. A gloomy general vision of mass climate migration, and particularly large flows from developing to developed countries, has motivated political authorities to devise early mitigation strategies. However, it is far from clear that migration is a first-order adaptation mechanism to cope with global warming.[2] Individuals of different origins, cultures, ages, education, income, and wealth levels are characterized by heterogeneous incentives and constraints that influence their propensity to flee damaged regions. In addition, those who decide to move are faced with a multitude of options, including local displacements, transitions to distant regions within their country of origin, or international relocation. Potential migrants must also face policy-related restrictions in reaching their destinations. The special report of the Intergovernmental Panel on Climate Change (IPCC) explicitly highlights the (relative) lack of knowledge about the long-run implications of CC on human migration: "Our understanding of the links of global warming to human migration are limited and represent an important knowledge gap" (Bindi et al. 2018). A better comprehension of CC-induced migration patterns is required, not only to anticipate future migratory pressures, but also to identify vulnerable populations that are likely to be trapped in extreme poverty and require specific interventions. All of the above-mentioned challenges constitute the motivation for this paper.

We set up a dynamic and micro-founded model of a rasterized world economy to shed light on the distributional consequences of CC, as well as on the size, structure, and spatial extent of climate migration that may be expected to occur during the rest of this century. We model migration decisions as an outcome of a random utility maximization (RUM) model that jointly accounts for the main migration mechanisms highlighted in the recent CC literature. We also keep track of the local context in

2. The literature documents that potential migrants from the poorest regions of the world are impeded by credit constraints and visa restrictions, implying that climate-driven economic losses could worsen their plight and lead to smaller international migration flows (Cattaneo and Peri 2016; Dao et al. 2018). Similarly, case studies conducted at the microeconomic level tend to confirm that internal migration responses are highly heterogeneous (e.g. Piguet 2010; Piguet, Pécoud, and De Guchteneire 2011; Gray and Mueller 2012; Bazzi 2017; Beine and Jeusette 2021) and difficult to predict.

which CC materializes and interacts with the characteristics of native populations. Compared with existing studies, our model's framework has the following advantages. First, we consider the three major dimensions of CC, namely changes in average surface temperatures (referred to as slow-onset (SO) changes), sea level rise (SLR), and extreme events and disasters (referred to as fast-onset (FO) shocks). Second, our model provides a detailed spatial representation of the world land surface divided into millions of pixels of 2.5 arc-minutes a side (about 5×5 km at the equator). This method allows us to model local damage from CC at an accurate resolution and to account for a fine spatial distribution of the world's population and economic activity. Third, the multi-stage RUM structure enables us to characterize the complex patterns of human migration. We model the long-term migratory responses to CC at various spatial scales, taking into account the interplay between alternative forms of migration, namely within national administrative areas (very-short-distance, referred to as *local*), within-country across administrative areas (short-distance, referred to as *regional*), and long-haul cross-border (long-distance, referred to as *international*). Fourth, heterogeneity in migratory behaviors is controlled by each locality hosting either of two sectors (agricultural and non-agricultural) populated by two types of agents (college graduates and the less educated) assigned to two age groups (young aged 0–30 and adult aged 30–60 years). Fifth, the dyadic structure of migration barriers across countries and regions allows us to control for the interactions between the legal, monetary, and psychological costs that individuals face when deciding to relocate. Rich data on the stocks of international and internal migrants allow us to identify migration cost parameters. Hence, our calibrated migration technology is arguably well-suited to yield plausible predictions of global migration patterns at a fine level of granularity. Finally, the endogenous migration decisions based on the comparison of attainable utility levels in all potential destinations are embedded in a general equilibrium framework. The direct and indirect effects of CC on human mobility, productivity, relative prices of goods, the global distribution of income, inequality, and extreme poverty are, therefore, jointly determined. Thus, the model is useful in investigating changes in migration policies that could affect the future global distribution of population, income, inequality, and poverty under various climatic scenarios.

Using this model of the world economy, we produce global migration and inequality responses to CC that are consistent with official Representative Concentration Pathways (RCPs).[3] Our main findings unfold as we incrementally add various incentives to migrate induced by different dimensions of CC. Focusing exclusively on SO factors (i.e. productivity changes due to rising temperature), we find a strong correlation between geographical latitude and climate-induced economic damage, with losses predominantly concentrated between the 20th parallels of north and south latitudes. Tougher economic conditions support voluntary displacement from lower- to higher-latitudes, as people substitute local or regional migration for international

3. As defined by the IPCC, RCP scenarios determine future trajectories of greenhouse gases concentration in the atmosphere. Hence, they serve as references for analyzing the variety of possible future states of the global climate.

migration. The consequential changes in total migration stocks are, however, limited. Then, adding SLR to the picture, we record significant increases in local and regional migration, as these two forms of relocation are more affordable for people forcibly displaced by CC. Apart from this direct consequence, SLR reduces the attractiveness of some highly developed and populated coastal areas. This has an indirect impact on the allocation of global migrants across destinations.

In our most comprehensive climate specification that adds FO factors, we observe significant changes in the world's socio-economic landscape. In our middle-of-the-road RCP7.0 scenario, global gross domestic product (GDP) shrinks by 9% in 2070 and by 12% in 2100 (and falls by 12% and 16% under RCP8.5, respectively). Africa, Asia, and South America are most affected by these losses, where GDP plunges by 40%, 25%, and 34%, respectively (by 52%, 33%, and 45%, respectively, under RCP8.5). Elsewhere in the world, more developed regions are hit by significantly smaller losses. For example, European GDP increases by 7% partly thanks to inflows of climate migrants. We find significant gaps in GDP losses between the RCP4.5 and RCP8.5 scenarios (the effects vary by a factor of 2), which clearly illustrate the huge (and hypothetically achievable) positive effect of implementing climate mitigation policies. We also find that CC accelerates urbanization, especially in developing countries, and raises the world's stock of human capital, as people tend to move from poorer regions to richer regions, where access to education is quasi-universal.

As to human migration, CC induces 45, 62, and 97 million working-age migrants of all education levels under RCP4.5, RCP7.0, and RCP8.5, respectively, over the course of the 21st century.[4] The variation across these three scenarios comes mainly from different levels of African and Asian emigration. Compared to those remaining in home countries, climate migrants are more educated (especially migrants leaving Africa), and tend to move longer distances, substituting within-country for cross-border movements. Under RCP7.0, we report international migration of 22 million people from Africa, 27 million from Asia, and 6 million from South America. These are small numbers from the point of view of the sending areas, indicating that international climate migration can be considered as a feasible adaptation strategy only for a small minority of affected populations. Conversely, from the point of view of the destination countries, these numbers are significant: Over the course of the 21st century, we predict an influx of 24 million climate migrants to Europe, 17 million to North America, and 5 million to Oceania. Nevertheless, it should be stressed that these are cumulative variations due to CC spread over three non-overlapping cohorts of people, which are rather small compared with the long-run international migration pressures caused by rising educational attainment and population growth differentials.

Overall, CC poses a threat to the quality of life, economic performance, and prosperity in many parts of the globe. It deepens the gap between developing and developed countries, between rural and urban areas, and also increases global poverty.

4. These numbers include only adults aged 30–60 years. Multiplying these cohorts by a factor of 2 gives a rough estimate of total population movements. These aggregate numbers are in line with Rigaud et al. (2018).

Under RCP4.5, RCP7.0, and RCP8.5, respectively, 7.5%, 9.5%, and 13% of the world's population falls below the relative threshold of extreme poverty (defined as 2% of the worldwide mean level of income in our model). Compared with 4% of the world's population living in extreme poverty if CC was absent, these increases reflect the higher toll of human suffering and indigence caused by the greenhouse effect. We also conclude that migration policies that do not take CC into account will not be an effective solution to mitigating the destructive effects of global warming. Neither opening country borders (by encouraging people to move) nor closing them (by retaining talent in poorer countries) is an efficient policy to alleviate the rise in extreme poverty induced by CC. Conversely, as explored by Burke, Hsiang, and Miguel (2015b) and Abel et al. (2019), CC will probably induce competition and conflicts over scarce and increasingly expensive resources and basic goods. Adding these potential conflicts to our computations exacerbates our already grim conclusions.

With this paper, we contribute to the growing literature on the links between CC and migration. Recent reviews of the empirical literature are provided in Millock (2015), Berlemann and Steinhardt (2017), Borderon et al. (2019), Cattaneo et al. (2019), and Hoffmann et al. (2020).[5] The literature has mostly looked at the short-term impact of FO variables (e.g. weather anomalies, hurricanes, extreme temperatures, torrential rains, floods, landslides, etc.), as opposed to long-run CC or SO mechanisms (e.g. temperature trends, desertification, rising sea levels, coastal erosion, etc.). While CC has consistently emerged as a potent driver of internal migration (Barrios, Bertinelli, and Strobl 2006; Piguet, Pécoud, and De Guchteneire 2011; Kubik and Maurel 2016; Thiede, Gray, and Mueller 2016; Dallmann and Millock 2017; Henderson, Storeygard, and Deichmann 2017; Deuster 2021; Castells-Quintana, Krause, and McDermott 2021; Peri and Sasahara 2019), the magnitude of these migratory responses varies drastically across these studies. With regard to international migration, the implications are far from precise. Some studies find important international migration outflows that are directly associated with weather shocks (Backhaus, Martinez-Zarzoso, and Muris 2015; Coniglio and Pesce 2015; Cai et al. 2016) or indirectly induced by CC-driven pressures on living standards in urban areas (Marchiori, Maystadt, and Schumacher 2012; Beine and Parsons 2015; Marchiori, Maystadt, and Schumacher 2017). Other papers attempt to explain why past migratory responses to climate shocks were small, non-existent, or even negative (Black et al. 2011, 2013; Grecequet et al. 2017; Cattaneo et al. 2019).[6] Recent studies focus on an individual's education level as an important

5. Earlier studies show that millions of people will migrate in the future as a result of CC (Gemenne 2011; Piguet, Pécoud, and De Guchteneire 2011). In response to the diversity of findings across studies, the paradigm has gradually changed, with recent studies seeing migration as one adaptation strategy among many (and not the least costly one).

6. Cattaneo and Peri (2016) report that a gradual increase in the temperature level reduces migration outflows from poor countries due to the presence of financial constraints. Bazzi (2017) finds similar results for Indonesia, as does Findley (1994) for Mali. The opposite finding occurs in studies conducted by Jayachandran (2006), Gray and Mueller (2012), and Mueller, Gray, and Kosec (2014), all of whom find that the migration response induced by CC is stronger among landless households than wealthy ones in India, Pakistan, and Bangladesh, respectively.

determinant for climate migration decisions (Helbling and Meierrieks 2021). Overall, methodological diversity is reflected in the heterogeneity of these findings. The meta-analyses in Beine and Jeusette (2021) and Hoffmann et al. (2020) identify a handful of important choices that might help explain the lack of conclusive findings that characterizes this broad literature.[7]

Our study is a part of an incipient literature pioneered by Desmet and Rossi-Hansberg (2015), Desmet, Nagy, and Rossi-Hansberg (2018), and Conte et al. (2021). All three studies quantify the economic consequences of CC by modeling the interactions across sector-specific productivity levels, human migratory patterns, and trade in a spatial context. In Desmet and Rossi-Hansberg (2015), all equilibria are spatially symmetric with prices and factor allocations identical for all uni-dimensional locations at a given latitude. Desmet, Nagy, and Rossi-Hansberg (2018) develop a two-dimensional spatial growth model, which Conte et al. (2021) extends by including a separate energy sector (thus, endogenizing carbon dioxide emissions).[8] Others (Costinot, Donaldson, and Smith 2016; Conte et al. 2021; Gouel and Laborde 2021), using spatial models, concentrate on agriculture by relying on crop yield estimates at a detailed spatial extent. As in these papers, we assume that every country is composed of a set of spatial units with various sectoral characteristics. But unlike these prior studies, we limit our analysis to two sectors (agriculture and non-agriculture), we disregard international trade, and we implement exogenous future CC scenarios. However, since we are looking for the first-order effects that CC may have on individual internal and international migration decisions, we use an improved migration predictive technology that incorporates the model's advantages enumerated above. This approach enables us to produce more detailed projections of migration stocks across all spatial locations in the world for the rest of the 21st century.

Another related study is by Shayegh (2017), who models the effect of CC on fertility rates, income inequality, and human capital accumulation in developing countries. He assumes that the probability of international migration is skill-specific, but that it increases exogenously with temperature changes, an assumption that leaves some micro-level interactions beyond the scope of the model. Similarly to Desmet and Rossi-Hansberg (2015), Shayegh (2017), and Conte et al. (2021), we endogenize the effects of temperature changes on productivity across different sectors. However, compared to these earlier studies, we use a more sophisticated migration technology and account for other CC-related effects, namely rising sea levels (Desmet et al. 2021), the damage that occurs due to natural disasters and extreme weather events (Drabo and Mbaye 2015; Heal and Park 2016), conflicts over scarce resources in poor countries (Abel

7. These choices are (i) the measurement of the dependent variable (international versus internal migration), (ii) environmental and economic factors considered (SO and FO direct and indirect effects), (iii) the geographical context and its scale, and (iv) methodology (most importantly, the identification strategy).

8. In follow-up papers, Desmet et al. (2021) use a similar methodology to simulate the impact of SLR on global development, while Cruz and Rossi-Hansberg (2021) analyze the role of various environmental policies on welfare.

et al. 2019), and migration policy scenarios (Benveniste, Oppenheimer, and Fleurbaey 2020).

Our model inevitably leaves out a number of relevant factors related to CC and future economic developments. Unlike the macro models of Nordhaus and Boyer (2000), Cruz and Rossi-Hansberg (2021), and Conte et al. (2021), carbon dioxide emissions are exogenously subsumed in the simulation scenario rather than treated as a result of explicitly modeled mitigation decisions. One reason for this choice is that the effects of population change on the concentration of greenhouse gases and the global mean temperature are highly uncertain (IPCC 2014, 2021). In addition, for a given emissions scenario, projections of climatic characteristics strongly vary across different climate models. We assume that CC and its direct impacts are exogenous to the economies under investigation. We also disregard the potential mitigation costs underlying the differences between our climate scenarios. It is worth noting that our results would remain unchanged if these costs involved universal taxes that are proportional to income (i.e. a uniform tax rate). We also keep climate-related policies constant, as if no investment in greener technologies took place. Finally, our model cannot cover the whole spectrum of CC-induced costs such as mortality/morbidity responses, effects on crime, or forced changes in consumer basket (Carleton and Hsiang 2016). Our model accounts only for those direct and indirect costs that can be calibrated using existing empirical studies and time-series data. Abstracting from these features enables us to develop a detailed spatial model with a special focus on the individual decision to migrate, the complex structure of destination choices, and the detailed distribution of ex-post population across space.

The rest of the paper is organized as follows. Section 2 describes our climate scenarios, discusses the construction of damage functions, and comments on the implications of three dimensions of CC, namely the SO, SLR, and FO mechanisms. Section 3 describes the theoretical model of the global economy used to predict the behavioral and market responses to CC. Section 4 shows the results of our climatic simulations obtained under various sets of assumptions. Section 5 presents counterfactual policy scenarios and discusses the implications of these alternatives for mitigating global inequality and poverty. Section 6 concludes.

2. Climate Change: Mechanisms and Damage

This section describes our climate scenarios for the 21st century, and the way we model the impact that global warming may have on the world's economy and people's well-being. We implement a high level of spatial geographic resolution, as the grid in our model considers pixel sizes of 2.5 arc-minutes per side, or about 5×5 km (3.1×3.1 miles) at the equator. The most comprehensive version of our model combines SO mechanisms, SLR, and FO mechanisms. The SO factors relate to changes in the monthly maximum values of temperatures and the impact of these temperature changes on industry-specific total factor productivity (TFP). The SO trends are easier for people to anticipate and are more likely to induce adaptation strategies such as crop

switching, firm reallocation, or voluntary migration. When adding the SLR mechanism, we use estimates of coastal flooding, and combine them with fine-grained population and topography data to predict forced displacement of populations living in low-elevation coastal areas and the share of land that is lost. Finally, the FO mechanisms account for expected utility and productivity losses induced by the increased frequency and intensity of extreme weather events and natural disasters. The modeling of the behavioral and market responses to these shocks will be developed in Section 3.

Our quantifications correspond to certain levels of carbon dioxide emissions determined by official RCPs. We consider RCP7.0 as our benchmark (or middle-of-the-road) scenario, whereas RCP4.5 and RCP8.5 delineate the spectrum of more optimistic and more pessimistic possibilities. Each RCP scenario is translated into consistent trajectories for SO, SLR, and FO variables at a fine-grained level. All three sets of climatic factors remain exogenous in our model, eliminating the uncertainty of endogenous CC-related links with economic activity, policies, carbon dioxide emissions, and implied changes in climate variables. For the sake of expository clarity, we introduce the SO, SLR, and FO channels sequentially, as each additional raster of climate shocks imposes distinct changes to the economic and migration effects projected by the model.

As far as the SO channel is concerned, there is a huge level of uncertainty surrounding the temperature responses to carbon dioxide emissions.[9] For each RCP scenario, we use monthly values of maximum temperature predictions from eight climate models. Uncertainty about SLR estimates is even larger because, among others, the dynamics of ocean heat uptake as well as the process of creation and decay of ice sheets and glaciers are difficult to predict. With regard to future FO events, we use our own series of regressions to predict the expected utility and productivity losses induced by natural disasters (i.e. droughts, floods, and storms) and heatwaves related to CC.

2.1. Slow-Onset Trends and Productivity Losses

We collect raw projections of monthly values of maximum temperature levels from WorldClim.org and link these data to the level of TFP in each spatial cell.[10] We consider

9. All climate models predict that CC will lead to a gradual rise in the mean surface temperature over the 21st century. However, not only does the exact impact of carbon dioxide emissions on magnitudes of global temperature changes remain uncertain. Potential environmental and economic damages induced by the same warming scenario across different climate models are subject to further uncertainty, as reviewed by Burke et al. (2015a).

10. Monthly values of maximum temperature are averaged over 20-year periods—2021–2040, 2041–2060, 2061–2080, 2081–2100—and are spatially downscaled at the resolution of 2.5 arc-minutes per side (approximately 5×5 km). For our various scenarios, we take the average values of eight global climate models published by WorldClim.org: BCC-CSM2-MR, CNRM-CM6-1, CNRM-ESM2-1, CanESM5, IPSL-CM6A-LR, MIROC-ES2L, MIROC6, and MRI-ESM2-0. Additionally, as a benchmark, we use historical monthly temperature records from WorldClim.org that cover the 2000–2010 period.

temperature projections from three RCP scenarios, and compare them with a no-CC hypothetical scenario:[11]

(i) RCP4.5 involves a warming of 2.5°C (4.5°F) in terms of the global average temperature, relative to the pre-industrial period 1850–1900, at the end of the 21st century.[12] It assumes a constant emission of carbon dioxide between 2020 and 2050, and carbon neutrality before 2100. We define RCP4.5 as our *optimistic scenario*, difficult to achieve unless fast and coordinated efforts result in reducing gross emissions in the coming decades.

(ii) RCP7.0 involves a warming of 3.5°C (6.3°F) in the global average temperature relative to the pre-industrial period, which corresponds to the scenario posited by the IPCC that keeps the pace of increase in greenhouse gases emissions approximately constant. We define RCP7.0 as our *benchmark scenario*.

(iii) RCP8.5 involves a warming of 4.5°C (8.1°F) in the global average temperature relative to the pre-industrial period. This corresponds to the most extreme scenario considered in the IPCC projections, assuming an increased pace of greenhouse gases emissions in the 21st century. We define it as our *pessimistic scenario*.

The map shown in the top panel of Figure 1 illustrates the distribution grid of daily temperature (averaged annually) across the world in 2010. The top-right panel presents latitude-specific mean levels of temperature. The bottom panel of Figure 1 depicts the changes in the average annual temperature predicted under the RCP7.0 scenario between 2010 and 2100, with latitude aggregates shown on the bottom-right panel. Note that the majority of the cells experience a temperature rise of more than 3°C (5.4°F), while the northern regions of Canada and Russia are projected to be almost 10°C (18°F) hotter than today. As expected, current temperature levels have strong negative correlation with latitude. However, the correlation between latitude and the predicted temperature change is lower, with small changes dominating regions just north of the equator as well as in some regions at high latitudes, both in the north and south hemispheres. Drastic changes in temperature levels are projected for the northern regions of Canada and Russia. Nonetheless, under RCP7.0, some densely populated regions in California, Mexico, the Great Lakes region, Eastern Europe, the Middle East, and Central Asia are predicted to suffer from above-average changes in mean temperatures.

The blue long-dashed and red dot–dashed lines in the bottom-right panel of Figure 1 show the latitude-specific changes in maximum temperatures obtained under two other RCP scenarios. The blue long-dashed line shows RCP4.5, and reveals that variations in temperature will be significantly below the ones projected in RCP7.0. All

11. The no-CC scenario is labeled RCP0.0 and assumes that there is no global warming in the 21st century, that is, temperatures are constant and correspond to the values observed in 2010.

12. Acknowledging the fact that in the decade of 2011–2020 the temperature has already gone up by 1.1°C (2.0°F) relative to pre-industrial period (IPCC 2021), the RCP4.5 scenario includes a further warming of 1.4°C (2.5°F).

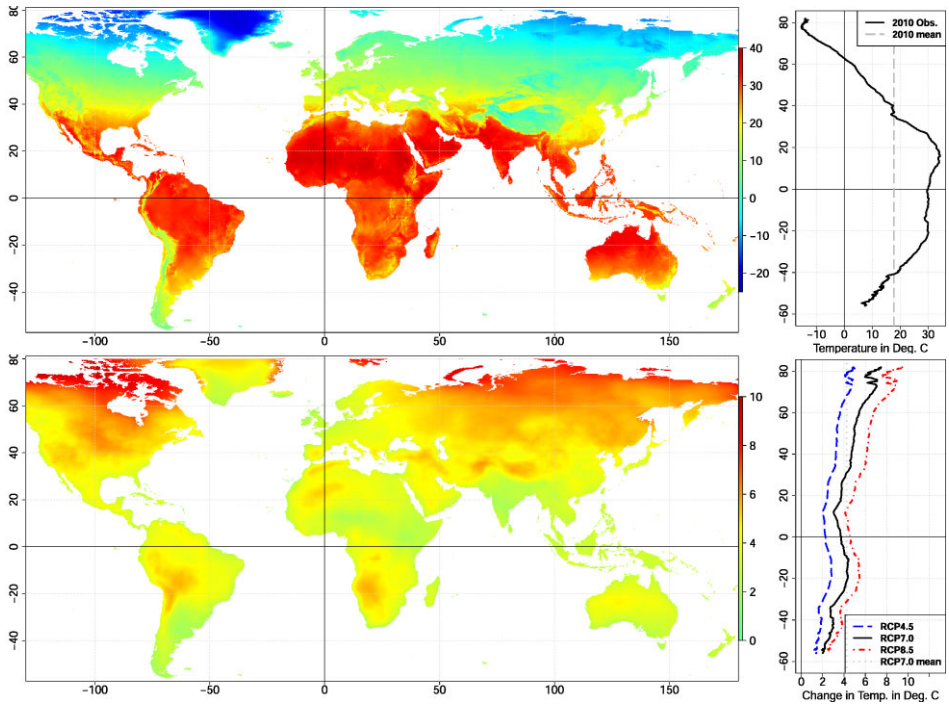

FIGURE 1. Average annual temperature in 2010 (top panel), and 2010–2100 variations in average annual temperature (bottom panel). The top panel depicts the spatial distribution of maximum temperature (annual average) across pixels (left panel) and across latitudes (right panel) in 2010. The bottom panel depicts the spatial distribution of changes in maximum temperature (annual average) in RCP7.0 in 2100 across pixels (left panel) and across latitudes (right panel). Data source: WorldClim.org.

latitudes are expected to experience an approximately uniform reduction in maximum temperatures of 1°C–1.5°C (1.8°F–2.7°F) relative to RCP7.0. A fast reduction in net carbon emissions might significantly lower the pressures from global warming, especially in already hot low-latitude areas, visibly constraining the extent of CC-induced damage in poorer countries. In contrast, the RCP8.5 scenario, depicted by the red dot–dashed line, lies within possible future outlooks for CC and predicts more pronounced warming at virtually all latitudes. The temperature level rises by 1°C–2°C (1.8°F–3.6°F) relative to RCP7.0 all over the world, which is expected to increase the damage and losses from CC in a nonlinear way.

In line with comparable studies (Desmet and Rossi-Hansberg 2015; Shayegh 2017; Conte 2020; Nath 2020; Desmet et al. 2021), we allow changes in temperatures to affect the level of TFP in agricultural and in non-agricultural sectors. To model the effect of temperature change, we follow Desmet and Rossi-Hansberg (2015), who estimate an inverted-U-shaped relationship between temperature (T) and TFP in the agricultural and manufacturing sectors. They include a quadratic scale factor $G_S^{SO}(T)$ in the TFP

of sector $S \in \{F, U\}$ that depends on the level of temperature. Desmet and Rossi-Hansberg (2015) define

$$G_S^{SO}(T) = \max\left\{g_{0S} + g_{1S}T + g_{2S}T^2; 0\right\},$$

where (g_{0S}, g_{1S}, g_{2S}) is a triplet of sector-specific parameters. If $g_{1S} > 0$ and $g_{2S} < 0$, the optimal temperature in sector S is given by $T_S^* = -g_{1S}/2g_{2S}$. Global warming increases the levels of TFP in localities with temperatures below T_S^*, while TFP decreases with temperature in places warmer than T_S^*.

Mendelsohn, Nordhaus, and Shaw (1994), Lobell and Burke (2010), and Carter et al. (2018) calibrate the quadratic relationship between TFP and temperature in the agricultural sector. To account for the possibility of adapting to CC by switching between crops, Desmet and Rossi-Hansberg (2015) estimate the envelope of the quadratic relationships obtained for different crops. This gives $(g_{0F}, g_{1F}, g_{2F}) = (-2.24, 0.31, -0.007)$, which determines an optimal temperature T_F^* of 21.1°C (70°F). This result also implies that agricultural yields are nil when temperature T_F is below 9.4°C (49°F) or greater than 32.9°C (91°F). The top panel of Figure 2 shows the relationship between temperature and agricultural productivity (in solid gray line), after smoothing $G_F^{SO}(T)$ with a Gaussian function to avoid negative productivity levels. The maximal productivity level is normalized to one.

To estimate the quadratic relationship in the non-agricultural sector, Desmet and Rossi-Hansberg (2015) use data on population density (a proxy for economic development) by latitude. They consider 1,000 bands of 9.6 km each and estimate the relationship between (smoothed) levels of population density and temperature. They obtain $(g_{0U}, g_{1U}, g_{2U}) = (0.3, 0.08, -0.002)$, which gives an optimal temperature T_U^* of 17.4°C (63°F).[13] Although the curve is flatter than in the agriculture sector, non-agricultural productivity is nil when temperature T_U is below −3°C (26.5°F) or above 38°C (100°F). The dashed black line in the top panel of Figure 2 shows the relationship between temperature and non-agricultural productivity after smoothing $G_U^{SO}(T)$ using a Gaussian function and normalizing the maximal productivity level to unity.

Finally, it is worth noting that we account for the anticipated variability in temperature during a year by computing monthly productivity losses due to CC before aggregating the monthly data to get the annual data. For each period t, month m, and pixel q, we plug in the average monthly levels of daily temperature, $T_{m,t}(q)$, in $G_S^{SO}(\cdot)$. We then compute the average of these monthly TFP levels for each period t:

$$G_{S,t}^{SO}(q) = \frac{1}{12}\sum_{m=1}^{12} G_S^{SO}(T_{m,t}(q)). \tag{1}$$

Recall from Figure 1 that the current maximum temperature levels are strongly correlated with latitude, whereas their expected variation under different RCP scenarios

13. On a similar note, Dell, Jones, and Olken (2014) show that industrial output decreases by 2% for a 1°C increase in temperature.

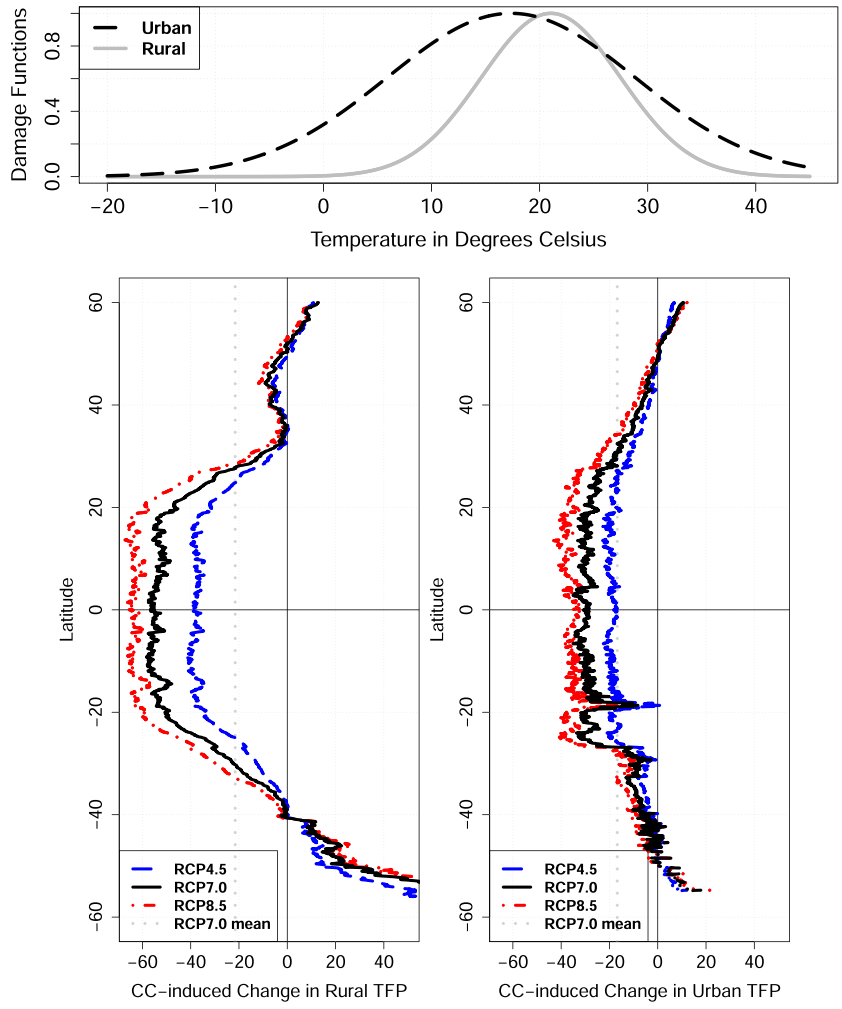

FIGURE 2. Damage functions due to SO CC and long-term productivity changes in 2100 by latitude. The top panel plots normalized Gaussian curves that fit damage functions for the agricultural (gray solid line) and the non-agricultural (black dashed line) sectors as functions of temperature (in degrees Celsius). In the two bottom panels, latitude is measured on the y-axis and sector-specific productivity changes in 2100 are measured on the x-axis (as the percent of deviation from RCP0.0, a no-CC scenario in 2100). The bottom-left panel illustrates changes in agricultural TFP, while the bottom-right panel depicts changes in non-agricultural TFP.

reveals only a weak correlation with latitude. More importantly, countries above the 40th parallel start out with temperatures below 20°C (68°F), while countries at lower latitudes have initial temperatures at much higher levels. Hence, similar variations in temperature values will induce dramatically different effects on productivity, depending on the geographical location of each pixel (which determines both $T(q)$ and $\Delta T(q)$). The bottom-left panel of Figure 2 depicts the predicted percentage

variations in agricultural productivity by latitude caused by projected changes in maximum temperatures in the year 2100. On average, in the RCP7.0 scenario (black solid line), agricultural productivity decreases significantly more than 50% in regions close to the equator. Agricultural productivity experiences more mitigated decreases (or even increases) at high latitudes. The bottom-right panel of Figure 2 shows the corresponding damage functions in the non-agricultural sector. On average, non-agricultural productivity decreases by 30%–40% in low-latitude areas and increases slightly at high latitudes. Both bottom panels of Figure 2 also give the predicted percentage variation in productivity implied by the RCP4.5 and RCP8.5 scenarios (the blue long-dashed and red dot–dashed lines, respectively). In both sectors, the productivity responses are strongly mitigated in the reduced emissions scenario, while they increase by approximately 10 percentage points at low latitudes in the RCP8.5 scenario.

In sum, the poorest regions of the world will be the most exposed to damage caused by the SO mechanism. The model shows that both rural and urban areas are likely to be affected, although the agricultural sector—dominant in developing regions—will suffer greater productivity losses. As it will be quantified later on, the mechanisms of CC-induced damage will severely increase global inequalities by widening the income gap between low- and high-income countries and will push the citizens of many developing regions into extreme poverty.

2.2. SLR, Forced Displacement, and Productivity Losses

Climate models predict that increasing global temperatures will lead to the melting of the Arctic, Antarctic, and continental ice caps. This will result in rising sea levels, coastal flooding, and the forced displacement of people living in low-elevation coastal areas (IPCC 2014, 2021).[14] There is great uncertainty about the magnitude of SLR because the dynamics of ocean heat uptake as well as the creation and decay of ice sheets and glaciers remain under intensive investigation. Furthermore, the positive feedback effects of reducing the Earth's surface albedo (causing further acceleration of heating) and lowering the stock of carbon dioxide accumulated in the oceans cannot be precisely predicted. Nonetheless, SLR will be an important factor that will certainly reshape the geography and economic potential of coastal regions all over the world (Hauer et al. 2020).

Our reference SLR estimates are taken from Jevrejeva et al. (2016) and Jackson and Jevrejeva (2016), who compute downscaled, 1-degree grids of the world's rising ocean levels that are consistent with RCP scenarios. Moreover, they provide confidence intervals at the 95% and 99% levels for each spatial cell. To deal with uncertainty surrounding SLR estimates, we take a conservative approach and use upper limits of these 95% ranges of SLR estimates in our model. Thus, we account not only for

14. Following the report by IPCC (Bindi et al. 2018): "The relative contributions from thermal expansion, glacier and ice-sheet mass loss, and freshwater storage on land [to SLR] are relatively well understood (Church et al. 2013; Watson et al. 2015) and their attribution is dominated by anthropogenic forcing."

the mean (expected) magnitude of SLR, but also for temporary and unpredictable sea level fluctuations that will deeply influence the livability of coastal areas. In the RCP7.0 scenario, the global mean sea level is expected to rise by approximately 0.7 m by 2100, with the 95% confidence interval being a 1-m rise.[15] However, the spatial heterogeneity in actual SLR is important, as some low-elevation zones of the world are more vulnerable to coastal flooding than other ones. Thermal expansion, ocean dynamics, and land ice loss will generate regional departures from the global mean SLR of about ±30% (Oppenheimer et al. 2019). Combining the SLR database with the elevation grid published by SEDAC (Berry, Smith, and Benveniste 2019) at the resolution level of 30 arc-second per side gives a very precise estimate of which areas are at risk of coastal flooding for different RCP scenarios, and what share of land will become unusable.

SLR induces two types of damage in our model. First, a fraction of the population living in low-elevation coastal zones is forcibly displaced, mechanically increasing the stock of climate migrants. We denote the fraction of the population that is forcibly displaced due to SLR in spatial cell q at period t as $\varphi_t(q)$, which is directly computed from the gridded data. Second, in flooded coast areas, SLR also induces losses in TFP that depend on the share of flooded land and implicit destruction of capital infrastructure. We denote the productivity loss due to SLR in spatial cell q at period t by $G_t^{SLR}(q)$, and assume that it is equivalent to the fraction of the forcibly displaced population, $\varphi_t(q)$. Therefore, SLR is bound to induce important geographic and economic changes in some of the world's coastal regions. Nevertheless, we allow the government to anticipate and mitigate these SLR-induced damages. In our reference scenario, we assume a 75% mitigation of SLR in high-income countries (i.e. in OECD and oil-producing countries in the Persian Gulf), as the authorities in many developed countries have recognized that SLR is a pressing issue (Haasnoot, Lawrence, and Magnan 2021; Horton et al. 2021; Moss et al. 2021).[16] In our model, this means that forced displacements and TFP losses from SLR cannot be higher than 25% in these countries. In contrast, we assume that SLR-related damage cannot be mitigated in developing countries, as they have little capacity to build technologically advanced barriers against SLR (Haasnoot, Lawrence, and Magnan 2021).

In aggregate terms, the RCP7.0 scenario projects a global sum of 47 million people affected by flooding due to SLR in 2100. Importantly, the optimistic RCP4.5 scenario reduces by 3.5 million the total number of people displaced by flooding caused by rising sea levels. As this number constitutes less than 8% of the world's population displaced by SLR in RCP7.0, the reduction of carbon emissions has little impact on SLR-induced damage due to a very high inertia of the oceanic system (Haasnoot, Lawrence, and Magnan 2021). However, in the most extreme RCP8.5 scenario, the

15. By 2100, the global mean magnitude of SLR equals 0.5 m (95% confidence interval at 0.85) under RCP4.5, and 0.8 m (95% confidence interval at 1.15 m) under RCP8.5.

16. Many localities around the world have already started implementing the integrated coastal zone management (ICZM) as their main SLR adaptation mechanism. The strategies focus on, among others, developing infrastructure, building walls, adjusting future city planning, and risk monitoring.

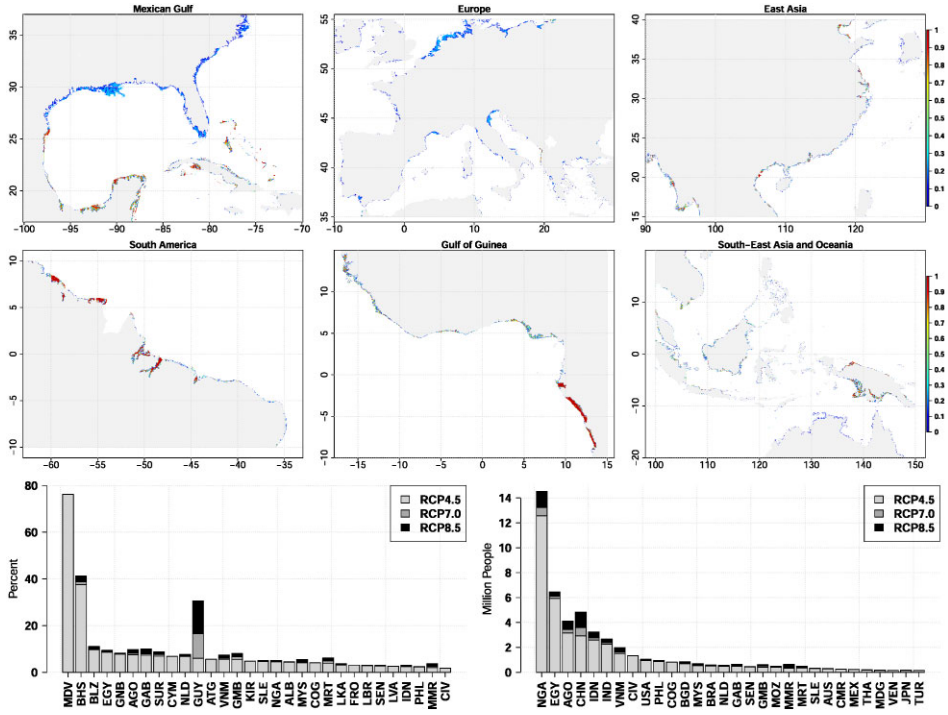

FIGURE 3. Forced displacement in 2100 due to rising sea levels under RCP7.0. The top panel plots six rasterized maps of flooded areas due to SLR for RCP7.0 in 2100. In order from left to right across the top half of the first panel, these include: the Atlantic coastline along the Southeastern United States and the Gulf of Mexico, Europe, and the East Coast of Asia. Along the bottom half of the first panel, these include the Northern Coast of South America, the Gulf of Guinea, and Oceania and the Southeast Asian Coastline. Colors of pixels reflect the fraction of land flooded, $\varphi_{2100}(q)$. The bottom-left panel summarizes 30 top countries in terms of the share of flooded population. The bottom-right panel summarizes 30 top countries in terms of the number of flooded people. Each country is labeled with its ISO code.

sum of flooded people goes up by 7.3 million. This is almost 15% more than the middle-of-the-road number, as global warming induces nonlinear SLR effects and the distribution of people with regard to elevation is nonuniform. Partly due to the construction to mitigate SLR, the highest positive deviations are predicted for the poorest countries. Nonetheless, SLR reinforces previous conclusions that CC has a strong impact on the global distribution of income and wealth, deepening inequality and poverty.

Figure 3 highlights spatial cells that will be totally or partially flooded in 2100 under our RCP7.0 scenario (top panel), and the numbers and shares of displaced people in most affected countries (bottom panels). Coastal areas around the Mexican Gulf, the Eastern United States, and Northern Europe are both highly populated and likely to experience flooding due to SLR. However, due to assumed mitigation capacity, these developed countries will suffer limited consequences of SLR in terms of the

population directly affected. In contrast, populations of many developing countries in Africa, Asia, and South America will be very vulnerable to SLR-induced forced displacement. According to the bottom panels of Figure 3, Nigeria, Egypt, Angola, China, India, and Indonesia are among the countries with more than 2 million people displaced due to floods caused by SLR. In relative terms, small islands such as the Maldives and the Bahamas are extremely endangered, followed by Belize, Guyana, Gabon, and Guinea-Bissau. The lack of potential mitigation capacity in these countries might generate further millions of forcibly displaced people who will migrate over short and long distances.

2.3. Fast-Onset Shocks, Productivity, and Utility Losses

While CC usually refers to long-term changes in mean temperature and sea levels, climatologists also predict changes in the frequency and intensity of extreme weather shocks that we classify into two categories, namely heatwaves and natural disasters, restricted to droughts, floods, and severe storms (IPCC 2021). The occurrence and incidence of these extreme weather events vary drastically across locations—implying that related economic costs are distributed in a very skewed way—and are virtually impossible to predict on daily basis. However, given the fact that one period in our model is meant to represent the active life of one cohort of individuals (i.e. 30 years), we rely on the law of large numbers to predict the intensity of FO shocks, and translate these shocks into expected productivity and utility losses in 2040, 2070, and 2100. We denote the productivity loss due to FO shocks in spatial cell q at period t as $G_t^{FO}(q)$. These parameters represent the share of GDP lost due to the expected intensity of FO factors, mapped in our model as losses in TFP. The utility losses, are modeled as uniform decreases in utility, and proxied by the share of people who are severely impacted by a weather-related shock induced by CC. These indicators represent the risk of incurring an arbitrarily large utility loss if people decide to stay in locations exposed to such events.

With regard to natural disasters, we collect data on the deciles of frequency and relative economic losses up to the year 2000 (Dilley et al. 2005). These data sets are published by SEDAC and document the distribution of losses and casualties generated from the EM-DAT database (Guha-Sapir 2009). To assign values to deciles, we construct the same distributions of economic and utility losses using the EM-DAT database (Guha-Sapir 2009). Combining these two data sources, we generate a spatial distribution of proportional economic and utility losses by pixels and by disaster type. We then use a series of own regressions to correlate the frequency and intensity of these losses with some moments of the regional temperature and precipitation distributions. We find empirical evidence that droughts are a function of precipitation in the driest quarter of a year, floods depend on precipitation in the wettest quarter, while storms derive from temperature levels in the wettest quarter. We estimate spatial fixed effect regressions of respective disasters on specific climatic variables, and project their intensity using future RCP-specific values of respective climatic factors. Finally, we aggregate all the damage into two measures of utility and economic losses.

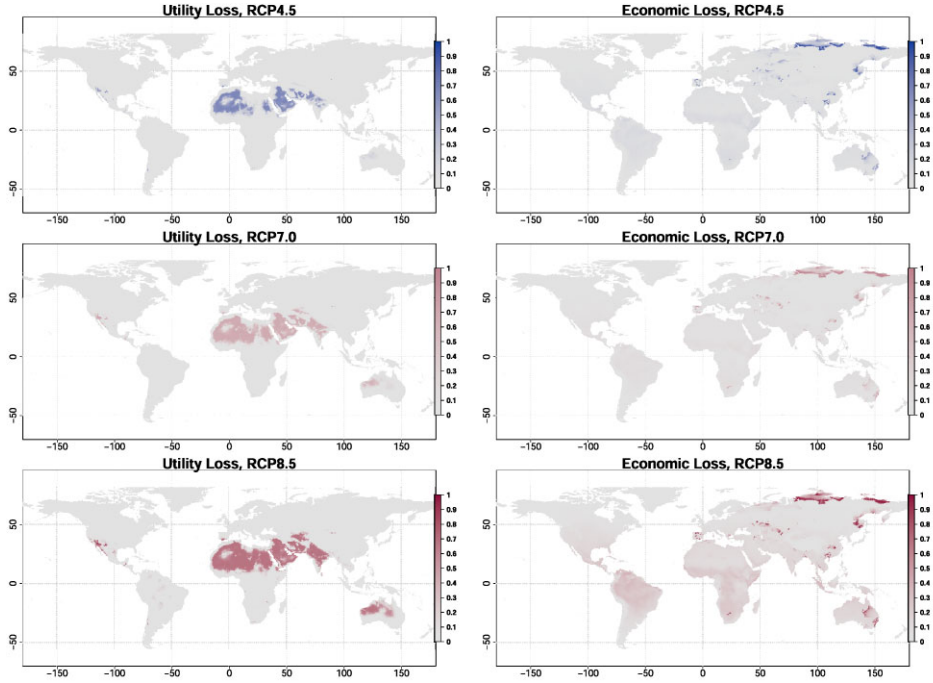

FIGURE 4. Utility and TFP losses generated by natural disasters and heatwaves in 2100. The three left-most maps plot utility losses incurred by people due to FO shocks under three scenarios: RCP4.5, RCP7.0, and RCP8.5. The three maps in the right-hand column depict productivity (i.e. economic) losses that occur under three different scenarios: RCP4.0, RCP7.0, and RCP8.5.

With regard to heatwaves, we follow Kjellstrom et al. (2019), who show that each day with a temperature above 25°C (77°F) is associated with a 25% lower productivity, while a day hotter than 35°C (95°F) implies an 80% drop in productivity (Heal and Park 2016). The number of days with temperatures exceeding 25°C and 35°C are directly obtained from the climateknowledgeportal.worldbank.org website and are available for all RCP scenarios and pixels. These productivity losses apply to all workers living in each spatial cell. Utility losses generated by extreme heat are calibrated using the EM-DAT distributions of people affected (Guha-Sapir 2009). Productivity losses due to heatwaves can be mitigated with air conditioning and other cooling technologies. In line with our treatment of coastal flooding, we assume that productivity losses are reduced by 75% in high-income countries, whereas such losses cannot be attenuated in developing countries.

Figure 4 shows utility and productivity losses by pixel (for a detailed exposition, refer to Online Appendix A.17). Heatwaves are the dominant FO factors, especially in Saharan Africa, Middle East, Central Asia, and Australia. Droughts prevail in California and the Mediterranean region, floods cause damage in northern Siberia, while severe storms become most prevalent in Japan, Madagascar, the Caribbean, and in Southern India. All in all, we predict moderate increases in the extensive and

intensive margins of droughts, floods, and storms. This finding is in line with climate projections about the future intensity and frequency of natural disasters (Bindi et al. 2018; IPCC 2021). However, heatwaves are going to be both more widespread and severe almost everywhere in the world (IPCC 2021). Even though the productivity losses from heatwaves are concentrated at low latitudes, in the future most areas of the world will suffer from substantial damage generated by heatwaves of larger magnitudes than the current ones. Similarly to our observations regarding SO and SLR, FO is also more concentrated among poorer and developing regions, inducing further adverse effects on global inequality and poverty.

3. Behavioral and Market Responses

Our priority in setting up the underlying general equilibrium model is threefold. First, we aim to represent the high degree of heterogeneity in exposure to CC across spatial cells. To this end, the model's detailed geographical structure includes 198 countries (denoted by $n \in N$), divided into 2,319 administrative regions (denoted by $r \in R$).[17] Furthermore, we divide each region into sub-locations, which are referred to as pixels or spatial cells, denoted by $q \in Q$. Each pixel is an approximate square of 2.5 arc-minutes (i.e. 5 km at the equator) per side, which yields more than 7,100,000 livable spatial cells worldwide, each of a surface at the equator of approximately 25 km^2 or 9.6 square miles. Second, we strive to capture the heterogeneity in individual relocation responses to CC. Thus, our model incorporates people of different ages (young and adult),[18] different origins, and two education levels (without a college degree, denoted by LS for low-skilled, and college graduates, denoted by HS for high-skilled). Education plays a key role in explaining differences in migration propensity between people because, among other things, education influences the dyadic (monetary, psychological, informational, and legal) costs of moving across countries, across regions within a country, or across pixels within a region. Third, we allow for CC to have a heterogeneous impact on productivity, given the type of sector that is dominant in a particular cell. Each pixel can be characterized as a rural or an urban area, hosting agriculture or manufacturing sectors, respectively. The model endogenizes productivity disparities across sectors and across pixels as a function of CC variables, educational levels of the resident workers, and residual time-invariant factors.

The choices to stay or to relocate are made by adults aged between 30 and 60 years. In making their decisions, they maximize a multi-stage random utility function by deciding where to live and how much to consume, taking migration costs, wages, and prices as given. As far as the location decisions are concerned, each adult decides whether to stay in the locality where she grew up, to move locally

17. By regions we mean first-level administrative areas, following Global Administrative Areas (GADM).

18. The model assumes 30-year-period overlapping-generations; for simplicity, we ignore the retirees.

within the same region, to emigrate to another region within the same country, or to move abroad to any of the 197 foreign countries. This choice depends on economic disparities across pixels, regions, and countries; on moving costs; and on external effects of population congestion. Fertility and education decisions are subsumed in exogenous socio-demographic scenarios.[19] Below, we present our theoretical model that maps CC-related damage into behavioral and market responses. We start with a description of production and migration technologies, define the model's inter-temporal equilibrium, and then summarize the principles of our calibration strategy.

3.1. Technology

We assume that output is proportional to labor in efficiency units.[20] Each pixel q belonging to the region $r \in R$ in country $n \in N$ is characterized by a production technology including two types of inputs: LS and HS workers (as in Vollrath 2009; Gollin, Lagakos, and Waugh 2014; Burzyński, Deuster, and Docquier 2020).[21] If pixel q is an urban type (U), then LS and HS are imperfect substitutes with an elasticity of substitution equal to σ. If q is a rural type (F), LS and HS workers are perfect substitutes, which implies a linear production function, and equal productivity of both skills. Free trade within each country ensures that the price of each good (U or F) is determined at the national level. The value of GDP assigned to pixel q equals the wage income of $q \subset r \subset n$ residents:

$$Y_U(q) = P_U(n) \cdot A_U(q) \cdot \left(mp^l(r) \cdot l(q) + mp^h(r) \cdot h(q)\right)$$

or

$$Y_F(q) = P_F(n) \cdot A_F(q) \cdot (l(q) + h(q)), \tag{2}$$

where $P_U(n)$ (or $P_F(n)$, respectively) is the price of the manufacturing (or agricultural, respectively) good in country n; $A_U(q)$ (or $A_F(q)$, respectively) denotes the pixel-specific TFP scale factor in sector U (or sector F, respectively); $l(q)$ and $h(q)$ are the number of LS and HS adult workers in q; and $mp^l(r)$ and $mp^h(r)$ are the TFP-deflated marginal products of LS and HS workers in an urban region r.

We assume that each pixel fully specializes in agricultural or manufacturing production, which determines whether the locality is a rural or an urban type. The

19. In a previous version of this paper, we endogenized fertility and parental decisions about children's education. However, we found that CC has little influence on before-migration population dynamics.

20. Such a model features a globalized economy with a common interest rate. Assuming a first-stage, Cobb–Douglas production function with physical capital (K) and composite labor (L), $Y_r = \hat{A}_r (K_r/L_r)^{\alpha} L_r$, and assuming that capital is internationally mobile with an exogenous international price of capital (R), $(K_r/L_r)^{1-\alpha} = (\alpha \hat{A}_r/R)$ would give $Y_r = A_r L_r$, where $A_r = \hat{A}_r^{1/(1-\alpha)} (\alpha/R)^{\alpha/(1-\alpha)}$ is a modified TFP level. This is in line with Kennan (2013) or Klein and Ventura (2009), who assume that capital "chases" labor over the long term, abstracting from variations in the international price of capital.

21. In what follows, we omit the time subscripts indicating the year in 21st century, $t \in \{2010, 2040, 2070, 2100\}$. Note, however, that all the model variables have a time dimension.

assignment of pixels to sectors is done endogenously, but not in a micro-founded way. We construct a three-step empirical algorithm that enables us to project the classification of pixels into rural and urban types. In a nutshell, we first determine the relationship between the intensity of urban activity and population density by running pixel-specific regressions with regional fixed effects. Then, we set up country-specific cutoffs of urbanization that determine the ranges of urban intensities for which rural and urban labels will be applied. Finally, we compute the maps of rural and urban pixels, by fitting our calibration to data published on urbanization rates.[22]

In the manufacturing sector, TFP is assumed to be equal to a product of three factors:

$$A_U(q) = G_U(q) \cdot (h(\tilde{q})/l(\tilde{q}))^{\varepsilon} \cdot \bar{A}_U(r), \tag{3}$$

where $G_U(q) \equiv G_U^{SO}(q) \cdot G_U^{SLR}(q) \cdot G_U^{FO}(q)$ combines the effects of SO, SLR, and FO climatic factors on TFP, as described in Section 2; the second term is a Lucas-type schooling externality, capturing the fact that college-educated workers facilitate innovation and the adoption of advanced technologies, with an elasticity of $\varepsilon \in (0, 1)$; the region-specific TFP residual $\bar{A}_U(r)$ reflects specific local factors such as the proportion of arable land, soil fertility, land ruggedness, regional amenities, institutional quality, etc.[23]

By analogy, for the rural sector, we have

$$A_F(q) = G_F(q) \cdot \bar{A}_F(r), \tag{4}$$

where $G_F(q) \equiv G_F^{SO}(q) \cdot G_F^{SLR}(q) \cdot G_F^{FO}(q)$, and $\bar{A}_F(r)$ is a residual productivity term.

Since we assume a constant elasticity of substitution (CES) production function in sector U, the TFP-deflated marginal products of LS and HS workers are endogenously determined according to available labor supplies. For each education level $i \in \{l, h\}$, we get

$$mp^i(r) = \frac{\partial}{\partial i(r)} \left(\eta(n) \cdot h(r)^{\frac{\sigma-1}{\sigma}} + (1 - \eta(n)) \cdot l(r)^{\frac{\sigma-1}{\sigma}}\right)^{\frac{\sigma}{\sigma-1}}, \tag{5}$$

where $\eta(n)$ is a country-specific relative productivity of college-educated workers (i.e. a skill bias in productivity), and σ is the elasticity of substitution between the two types of workers.

Note that in our model, labor markets are region-specific, but wage rates are pixel-specific. The former implies that the TFP-deflated marginal productivity of labor depends on the total supply of workers available in region r, whereas the latter allows

22. Details of this procedure can be found in Online Appendix B.

23. Note that the Lucas externality considers the level of human capital available in the pixel q and the surrounding pixels, denoted as $\tilde{q}$. We make this assumption, as commuting zones are rarely constrained by people's place of residence. Consequently, $\tilde{q}$ includes all the pixels in the radius of 20 km from q, weighted proportionally to distances.

for local changes in TFP due to skill abundance and climate variability. As a result, for every pixel q, the wage rates in both sectors are determined by the good-specific price levels, the TFP levels, and marginal productivity of labor. These conditions yield

$$w_U^l(q) = P_U(n) \cdot A_U(q) \cdot \left(\eta(n) \cdot h(r)^{\frac{\sigma-1}{\sigma}} + (1-\eta(n)) \cdot l(r)^{\frac{\sigma-1}{\sigma}}\right)^{\frac{1}{\sigma-1}} \cdot \frac{1-\eta(n)}{l(r)^{1/\sigma}},$$

$$w_U^h(q) = P_U(n) \cdot A_U(q) \cdot \left(\eta(n) \cdot h(r)^{\frac{\sigma-1}{\sigma}} + (1-\eta(n)) \cdot l(r)^{\frac{\sigma-1}{\sigma}}\right)^{\frac{1}{\sigma-1}} \cdot \frac{\eta(n)}{h(r)^{1/\sigma}},$$

or

$$w_F^l(q) = w_F^h(q) = P_F(n) \cdot A_F(q), \tag{6}$$

so that the urban wage ratio between HS and LS workers in pixel $q \subset r \subset n$ is given by

$$\omega(r) = \frac{w_U^h(q)}{w_U^l(q)} = \frac{\eta(n)}{1-\eta(n)} \cdot z(r)^{\frac{-1}{\sigma}}, \tag{7}$$

where $z(r) \equiv h(r)/l(r)$ is the skill ratio in employment in region r.

As far as the skill bias, $\eta(n)$, is concerned, we assume directed technical change that affects different types of workers in a non-uniform way. As technology improves, the relative productivity of college-educated workers increases, particularly in the non-agricultural sector (Acemoglu 2002; Restuccia and Vandenbroucke 2013). For example, Autor, Levy, and Murnane (2003) show that computerization is associated with declining the relative demand for routine manual and cognitive tasks and increasing the relative demand for non-routine cognitive tasks. The observed relative demand shift favors college-educated versus non-college-educated labor, which implies

$$\frac{\eta(n)}{1-\eta(n)} = \bar{\eta} \cdot z(n)^{\kappa}, \tag{8}$$

where $\bar{\eta}$ is an exogenous term, $\kappa \in (0,1)$ is the elasticity of skill bias with respect to the skill ratio in the urban sector, and $z(n)$ is a country-specific skill ratio. Given data on wages by skill levels across countries, equations (7) and (8) enable us to identify the value of parameter κ given the wage premium and labor force data.

3.2. Individual Choices

Each adult faces a sequential decision process under full information. First, she has to determine the optimal structure of consumption under market and budgetary constraints. This choice results in setting the values of *inner utility* functions by pixel. Second, every decision maker chooses a preferred place of residence, subject to predetermined migration costs. Individuals follow the RUM principle, and determine the values of their *outer utility* functions by pixel, given a set of deterministic characteristics

of all potential destinations, and a collection of individual-specific idiosyncratic taste shocks.

3.2.1. Consumption Decisions. Individuals have homothetic, CES preferences over two consumption goods. The utility from consuming agricultural and manufacturing goods by an individual of education level $i \in \{l, h\}$ living in pixel $q \subset r \subset n$ equals

$$c^i(q) = \left(c_F^i(q)^{\frac{\rho-1}{\rho}} + \theta(n) \cdot c_U^i(q)^{\frac{\rho-1}{\rho}}\right)^{\frac{\rho}{\rho-1}}. \tag{9}$$

In this setup, ρ is the elasticity of substitution between agricultural and manufacturing goods, while $\theta(n)$ is a country-specific preference parameter for manufacturing goods. Function (9) is maximized subject to a standard budget constraint for given price levels $P_F(n)$, $P_U(n)$, and individual-specific wage rate $w^i(q)$:

$$P_F(n) \cdot c_F^i(q) + P_U(n) \cdot c_U^i(q) = w^i(q). \tag{10}$$

This *inner utility* maximization problem solves as

$$\begin{aligned} c_F^i(q) &= P_F(n)^{-\rho} \cdot P(n)^{\rho-1} \cdot w^i(q), \\ c_U^i(q) &= \theta(n)^{\rho} \cdot P_U(n)^{-\rho} \cdot P(n)^{\rho-1} \cdot w^i(q), \end{aligned} \tag{11}$$

where $P(n) = (P_F(n)^{1-\rho} + \theta(n)^{\rho} \cdot P_U(n)^{1-\rho})^{\frac{1}{1-\rho}}$ is the country-specific ideal price index. Note that the former expressions imply that for each pixel q, the utility individual i derives from consumption equals $c^i(q) = w^i(q)/P(n)$.

Assuming that the price of manufactured goods in every country is the *numéraire*, we show that the parameter of relative preference for manufactured goods is a function of their share in total expenditures, $s_U(n)$, and the price index: $\theta(n) = (s_U(n) \cdot P(n)^{1-\rho})^{1/\rho}$. This allows us to identify parameters $\theta(n)$, given the data on the consumption share of manufacturing goods and a cross-section of purchasing power parity (PPP) indicators. In our projections, for a given endogenous structure of consumption, $s_U(n)$, we set n-specific agricultural goods price levels to

$$P_F(n) = \theta(n)^{\frac{\rho}{1-\rho}} \cdot \left(\frac{1 - s_U(n)}{s_U(n)}\right)^{\frac{1}{1-\rho}}. \tag{12}$$

3.2.2. Migration Decisions. Individual migration decisions are motivated by the comparison of discrete alternatives: staying in the pixel of birth, emigrating to another pixel within the home region, moving to a different region within a person's native country, or emigrating to a foreign country. To model these decisions, we use a logarithmic *outer utility* function with a deterministic and a random component. The utility of an adult of type i, born in pixel $q \subset r \subset n$, moving to pixel $q' \subset r' \subset n'$, depends on three deterministic factors: (i) the real wage rate attainable in q' for education level i, (ii) the i-specific migration cost of moving between q and q', and

(iii) the congestion externality related to the total population residing in q'. Additionally, each individual's *outer utility* function incorporates a random utility component, $\xi^i(q')$ representing idiosyncratic tastes for living in pixel q'. This variable follows an i.i.d. extreme value (EV) type I distribution (i.e. the Gumbel distribution) with a normalized mean and scale. Overall

$$u^i(q,q') = \alpha^i \ln \frac{w^i(q')}{P(n')} + \ln(1 - x^i(q,q')) + \delta \ln(l(q') + h(q')) + \xi^i(q'), \quad (13)$$

where $\alpha^i > 0$ is the education-specific elasticity of utility with respect to real wage rate, while $\delta < 0$ measures the magnitude of disutility from congestion.[24]

Migration costs are exogenous, and they vary across location pairs, education levels, and the three types of migration. In particular,

$$\begin{aligned} &\text{if} \quad q' \subset r/q, \quad \text{then} \quad x^i(q,q') = x^i(r), \\ &\text{if} \quad q' \subset n/r, \quad \text{then} \quad x^i(q,q') = x^i(r,r'), \\ &\text{if} \quad q' \not\subset n, \quad \text{then} \quad x^i(q,q') = x^i(n,n'). \end{aligned} \quad (14)$$

Equations (14) include three options to migrate. First, we consider a situation in which a person moves locally, within her administrative region of birth. In that case, a scalar, region-specific migration cost applies. Second, $x^i(r,r')$ represents the regional migration options, in which a person chooses any pixel within her country of birth outside her region of birth. In that case, region-pair-specific migration costs apply. Finally, cross-border movements are included in $x^i(n,n')$; international migration costs take a country-pair-specific form in case of choosing q' outside a person's country of birth.[25]

3.2.3. Migration Aggregates. Following McFadden (1974), the assumptions about the distribution of random utility components (namely, EV distribution and independence) allow us to write the individual probabilities of choosing any destination $q' \subset r' \subset n'$, conditional on originating from $q \subset r \subset n$ as[26]

24. Similarly, δ might be interpreted as an exogenous way of modeling any other deglomeration force, such as increasing real estate prices in crowded localities.

25. This structure of migration costs implies that international migrants do not face regional or local migration costs. Consequently, the choice of a specific region and pixel after moving across country borders is done by comparing region-specific and pixel-specific expected utilities, respectively. The same applies to local migration costs and pixel choices when moving regionally.

26. The expected value of an EV Type I distributed random utility over a choice set N equals $\mathbb{E}[u(N)] = \ln(\sum_{p \in N} \exp u(p))$. The expression to the right is often called the inclusive value of utility, or simply the log-sum. We use this property of the Gumbel distribution in moving from line two to line three of the derivation in equation (15).

$$
\begin{aligned}
\Pi^i(q,q') &= \frac{\exp u^i(q,q')}{\sum_{p_q \subset N} \exp u^i(q,p_q)} \\
&= \frac{\exp u^i(q,q')}{\sum_{p_q \subset r'} \exp u^i(q,p_q)} \cdot \frac{\sum_{p_q \subset r'} \exp u^i(q,p_q)}{\sum_{p_q \subset n'} \exp u^i(q,p_q)} \cdot \frac{\sum_{p_q \subset n'} \exp u^i(q,p_q)}{\sum_{p_q \subset N} \exp u^i(q,p_q)} \\
&= \frac{\exp u^i(q,q')}{\sum_{p_q \subset r'} \exp u^i(q,p_q)} \cdot \frac{\exp \mathbb{E}[u^i(r')]}{\sum_{p_r \subset n'} \exp \mathbb{E}[u^i(r,p_r)]} \\
&\quad \cdot \frac{\exp \mathbb{E}[u^i(n')]}{\sum_{p_n \subset N} \exp \mathbb{E}[u^i(n,p_n)]} \\
&= \pi^i(q'|r') \cdot \pi^i(r'|n') \cdot \pi^i(n'|n),
\end{aligned}
\tag{15}
$$

where $p_q \subset r'$ denotes all the pixels in the region of destination r', $p_r \subset n'$ denotes all the regions in the country of destination n', and $p_n \subset N$ denotes all the countries in the choice set.[27]

The last step derives from the definitions of migration costs in equation (14):

$$
\begin{aligned}
u^i(q,q') &= \begin{cases} u^i(q') + \ln(1 - x^i(r)) \iff q' \subset r, \\ u^i(q') + \ln(1 - x^i(r,r')) \iff q' \subset n/r, \\ u^i(q') + \ln(1 - x^i(n,n')) \iff q' \nsubseteq n, \end{cases} \\
u^i(q,p_q) &= \begin{cases} u^i(p_q) + \ln(1 - x^i(r)) \iff p_q \subset r, \\ u^i(p_q) \iff p_q \nsubseteq r, \end{cases} \\
\mathbb{E}[u^i(r,p_r)] &= \begin{cases} \mathbb{E}[u^i(p_r)] + \ln(1 - x^i(r,p_r)) \iff p_r \subset n, \\ \mathbb{E}[u^i(p_r)] \iff p_r \nsubseteq n, \end{cases} \\
\mathbb{E}[u^i(n,p_n)] &= \begin{cases} \mathbb{E}[u^i(n,p_n)] + \ln(1 - x^i(n,p_n)) \iff p_n \neq n, \\ \mathbb{E}[u^i(p_n)] \iff p_n = n. \end{cases}
\end{aligned}
\tag{16}
$$

Equation (15) indicates that the migration choice can be decomposed into three conditional probabilities of choosing: (i) the country n', conditional on residing in n, (ii) the region r', conditional on having selected n' as the destination country, and (iii) the pixel q', having selected region r' as the preferred destination. All of the conditional choices depend on region- and country-specific expected utilities, which enables us to compute emigration and immigration probabilities by pixel, region, and country. Overall, an individual's migration choice set comprises

27. As explained in Online Appendix A.11, the final computation of expected utilities also includes pixel weights. This assumption allows us to attenuate the importance of low-populated, least-attractive pixels, which (unless weighted) enter the computation of expected utilities symmetrically to highly populated and attractive cells. Online Appendix D.1 provides a robustness check of our results with respect to this assumption.

$\mathcal{N} = 1 + 1 + R_n - 1 + N - 1 = R_n + N$ options.[28] The model fulfills the independence of irrelevant alternatives (IIA) axiom, implying that for any triplet q, q', q'', the ratio of choice probabilities $\Pi^i(q, q'')/\Pi^i(q, q')$ depends solely on the economic characteristics of q' and q'', as well as the bilateral migration costs $x^i(q, q')$ and $x^i(q, q'')$, but not on the features of all other options available in the choice set.

3.2.4. Forcibly Displaced Individuals and Utility Losses Due to Disasters. The fraction of people whose home (birthplace) gets flooded in t due to SLR is given by $\varphi_t(q)$ as defined in Section 2. These individuals have no other option but to move. Therefore, their migration choice set is more limited, as staying in the pixel of birth is not allowed. Consequently, for every forcibly displaced i-type individual from pixel q, equation (15) gets modified because $u^i(q, q) = 0$. Since mobility costs increase with distance, less expensive local movements are expected to increase the most, as only a fraction of forcibly displaced people can afford to move across regions or country borders.

Technically, we assume that SLR has a uniform impact on all individuals living in the flooded pixels. In coastal pixels that are completely flooded, we also assume that production capacity is totally destroyed, by lowering the pixel-specific TFP level to zero. However, the majority of pixels in our model are partially flooded (flooded in a proportion $\varphi_t(q)$ between 0 and 1). In such cases, we assume that both people and production capacity are uniformly distributed within a partially flooded pixel q. As such, a fraction $\varphi_t(q)$ of people gets forcibly displaced, while a share $1 - \varphi_t(q)$ of the pixel-specific TFP survives the SLR. The latter effect is included to proxy the damage caused by capital destruction. In this way, SLR also generates potential for further voluntary migration movements, as for the population share of $1 - \varphi_t(q)$, the incentives to remain in any partially flooded pixel are reduced when TFP decreases and expected wage rates are cut.

In the same vein, we assume that utility losses generated by FO factors uniformly reduce the utility of living in any affected pixel q by $\varphi_t(q)$. It corresponds to assuming that with probability $\varphi_t(q)$ utility $u^i(q, q)$ reduces to zero, while it remains unchanged with probability $1 - \varphi_t(q)$.

3.3. Dynamics and Inter-Temporal Equilibrium

In each moment t, we can characterize the equilibrium structure of the resident population of type $i \in \{l, h\}$ in each pixel $q \subset r \subset n$ of the world, by summing all local, regional and international migrants and adding them to the population of

28. That is, one option is to stay in the domestic pixel, one option is to move locally within the domestic region (and then be assigned to a pixel based on the comparison of expected utilities), $R_n - 1$ options are to move regionally (and be assigned to a pixel based on the comparison of expected utilities), and $N - 1$ options are to move internationally (followed by an assignment to a respective region and pixel as a result of expected utility comparison).

stayers in q:

$$l_t(q) = \hat{l}_t(q) \cdot \left(1 - \sum_{p_q \subset N/q} \Pi_t^l(q, p_q)\right) + \sum_{p_q \subset N/q} \Pi_t^l(p_q, q) \cdot \hat{l}_t(p_q),$$

$$h_t(q) = \hat{h}_t(q) \cdot \left(1 - \sum_{p_q \subset N/q} \Pi_t^h(q, p_q)\right) + \sum_{p_q \subset N/q} \Pi_t^h(p_q, q) \cdot \hat{h}_t(p_q), \quad (17)$$

where $(\hat{l}_t(q), \hat{h}_t(q))$ denote the pre-migration population of LS and HS workers in time t in pixel q. The latter is computed using exogenously given region- and skill-specific fertility rates $f_t^i(r)$ and region- and skill-specific probabilities of obtaining higher education $p_t^i(r)$:

$$\hat{l}_{t+1}(q) = l_t(q) \cdot f_t^l(r) \cdot \big(1 - p_t^l(r)\big) + h_t(q) \cdot f_t^h(r) \cdot \big(1 - p_t^h(r)\big),$$
$$\hat{h}_{t+1}(q) = l_t(q) \cdot f_t^l(r) \cdot p_t^l(r) + h_t(q) \cdot f_t^h(r) \cdot p_t^h(r). \quad (18)$$

With this final dynamic condition, the inter-temporal equilibrium for the world economy can be defined as follows:

DEFINITION 1. Assume a given geographical structure of the world economy, comprising N countries, R regions, and Q pixels, as well as a respective assignment of pixels to regions, and regions to countries. For a set $\{\sigma, \kappa, \varepsilon, \alpha^i, \rho, \delta, \bar{\eta}\}$ of common parameters, a set $\{\theta(n), P_{U,t}(n) = 1, \bar{A}_U(r), \bar{A}_F(r), x^i(r)\}$ of country- and region-specific exogenous characteristics, a set of predetermined dynamic region-specific characteristics $\{f_t^i(r), p_t^i(r)\}$, matrices of regional and international migration costs $\forall n, n' \forall r, r' \subset n$, $x^i(r, r'), x^i(n, n')$, predetermined CC scenarios, and initial conditions on population and education distribution across all pixels $\{i_{2010}(q)\}$, an inter-temporal equilibrium is a set of economic $\{Y_{U,t}(q), Y_{F,t}(q), A_{F,t}(q), A_{U,t}(q), \eta_t(n), P_{F,t}(n), w_{U,t}^i(q), w_{F,t}^i(q), c_t^i(q)\}$ and demographic $\{\hat{h}_t(q), \hat{l}_t(q), h_t(q), l_t(q)\}$ endogenous variables, which simultaneously satisfies technological constraints (2), (3), (4), and (8); prices and wages (6) and (12); consumption decisions (11); utility across pixels and migration probabilities (13) and (15); and the dynamics of the population (17) and (18).

3.4. Data and Calibration

In this subsection, we summarize the principles of our calibration strategy. Details about the calibration of the benchmark model as well as a sensitivity analysis based on alternative parameter values can be found in the Online Appendices A and D, respectively. The main strategy is to use all the degrees of freedom of the data to identify the needed coefficients, implying that our model is exactly identified for year 2010.

Socio-Economic Data Sources. Our model needs to be supplied with several pixel-specific data sets. We collect the high-resolution data on (i) population and age structure by pixel from WorldPop.org (Lloyd, Sorichetta, and Tatem 2017), (ii) distribution of education by pixel from the Institute for Health Metrics and Evaluation (IHME 2020), (iii) urbanization of pixels from WorldPop.org (Nieves et al. 2020), and (iv) the pixel-specific GDP estimates from Kummu, Taka, and Guillaume (2018). Additionally, we use country-specific data on (i) fertility projections from the UN Population Division, (ii) education wage gaps from Global Jobs Indicators Database (JoIn) by the World Bank, (iii) GDP levels and shares of agriculture in consumption and PPP rates from the World Bank, and (iv) shares of HS population from Barro and Lee (2013). These data sets are the primary sources for our region-specific imputations. We collect international migration data by skill level from the OECD DIOC-E database (and we impute the South-South migration stocks using the UN Population Division data set). The DIOC-E database relies on census and register data, implying that it badly captures undocumented immigration. Finally, country-specific regional migration stocks by education levels are constructed using census data (IPUMS International), the WorldPop.org data (Sorichetta et al. 2016), and the Labor Force Survey data by Eurostat. These combined data sets allow us to compute pixel-specific populations by skill level and age, TFP residuals, and ultimately wage rates by pixel and by education level.

Model Parameters. In our benchmark simulations, we set some common parameters to values postulated by the literature. The elasticity of substitution between college graduates and less educated workers in all urban pixels equals $\sigma = 2$, following Ottaviano and Peri (2012). Vollrath (2009) and Lucas (2009) state that skill groups are perfect substitutes in the agricultural sector. The elasticity of substitution between agricultural and manufacturing goods is set to $\rho = 4$, following Feenstra, Inklaar, and Timmer (2015). Other parameters are determined using regressions. We calibrate the skill-bias terms, $\eta(n)$, and respective elasticity, $\kappa = 0.41$, by regressing observed wage gaps on the skill ratio across countries. The magnitude of the technological externality $\varepsilon = 0.28$ is calibrated using data on country-specific populations by education and GDP levels in 2000 and 2010. The congestion externality, $\delta = -0.04$, is estimated using changes in pixel-specific populations between 2000 and 2010, controlling for wage differences. Finally, we compute elasticities of outer utilities with respect to wage rates by constructing gravity-like migration equations by country-pair and skill level. This approach gives $\alpha^l = 0.44$ and $\alpha^h = 0.86$, which are in line with estimates on international migration (Bertoli and Fernández-Huertas Moraga 2013). With these values, we can set all international and regional migration cost parameters, by using all degrees of freedom given the respective migration matrices in 2010.

Projection Parameters. As far as projections are concerned, we use pre-determined paths for fertility and higher education probabilities that originate from regional interpolations and temporal extrapolations of 2010 data. We regress observable data

points of $f^i_{2010}(n)$ and $p^i_{2010}(n)$ on country-specific GDP per capita. We take country-specific residuals as fixed effects for regional interpolations of these variables for 2010. Finally, in each future period, we keep the country-fixed effects and estimated parameters constant, and we determine future values of both variables by supplying the econometric model with future GDP per capita computations. We also project the sector type for all pixels. To this end, we regress 2010 urbanization, as well as UN projections for urbanization in 2040, on pixel-specific population stocks with country fixed effects. Ultimately, we project each pixel's type using the model's population projections and estimated parameters. Future values of pixel-specific damage functions are easily computed using RCP scenario-specific predictions of temperatures by pixels. Local, regional, and international migration costs are assumed to be constant at their 2010 level throughout the 21st century.

4. Results

In Section 4.1, we focus on SO mechanisms (i.e. changes in TFP that occur due to rising temperatures) and analyze these implications for projecting global trends in economic performance and migratory patterns over the remaining decades of the 21st century. Then, we add to these baseline predictions by accounting for TFP losses and forced displacement due to SLR in Section 4.2. Finally, Section 4.3 discusses the results obtained when using the most comprehensive version of the model, which accounts for the increased frequency and intensity of FO shocks, alongside SO mechanisms and SLR. The robustness of our results is investigated in the Online Appendix D.

4.1. Slow-Onset Mechanisms

Humans have known about the dangers of global warming for decades, if not a century. However, because the effects have been so slow in unfolding, at least up until the 1980s, there has been a delayed policy response. Today, the scientific evidence is clear: The SO factors are speeding up and much of this change will be irreversible. In this subsection, we analyze the worldwide effects that changes in temperatures will have on local, regional, and cross-border migration, as well as on income per capita, human capital distribution, and urbanization patterns. In line with Section 2.1, SO CC factors affect TFP through the temperature channel, and this impact varies across geographical space and industries. Due to high initial temperature levels in low-latitude areas, a relatively low magnitude warming induces significant losses. Hence, the risk of incurring substantial negative effects from SO factors is high between tropics. These macro regions house a large fraction of the world's population, although the economies in these areas contribute less to global GDP than countries located in higher latitudes. In contrast, high-latitude areas (such as Siberia or Scandinavia) are expected to gain from increasing temperatures as warming brings them neutral or positive impacts on productivity and might improve living conditions. Economies in high latitudes are

relatively richer, and account for a large share of the world's GDP, which mitigates the global economic losses due to the increase in temperatures.

Rural regions are particularly exposed to temperature changes, almost twice as much as urban areas (compare the bottom-left and bottom-right panels of Figure 3). Agriculture accounts for a large share of employment and income in developing economies, and this sector incurs substantial losses from global warming. Overall, CC increases TFP disparities between countries and regions, mostly harms the world's poorest residents and exacerbates global income inequality. As the population residing in the developing world is concentrated in rural areas, CC implies a non-negligible reallocation of people from lower-productivity rural to higher-productivity urban localities in less-developed economies. While migration of some sort has always been a response to existing economic disparities, CC causes people to increase the distance of their migratory movements. This is because temperature shocks are spatially correlated. The expected utilities in nearby localities co-move and the future attractiveness of short-distance migration movements decreases relatively to longer distance moves. Therefore, people tend to substitute local for regional migration, and trade regional for international migration.

Table 1 illustrates these key findings. Results are expressed as deviations in the main macroeconomic aggregates from a hypothetical no-CC scenario (RCP0.0 base case, in which all climate variables are kept at their 2010 levels throughout the 21st century). We report the deviations in 2040, 2070, and 2100 for the three RCP scenarios, and we provide a decomposition of the global responses by continent. Looking at the first set of columns, in the poorest regions of the world, CC induces a massive and negative macroeconomic shock. In RCP7.0, the middle-of-the-road scenario, Africa, Asia, and South America lose up to 35% of GDP, both due to direct productivity losses and to voluntary international emigration. Disregarding the cost of SLR and FO shocks at this stage, developed regions in general, and European countries in particular, see their GDP increase. In the second part of the century, SO factors contribute to a dramatic loss of productive capacity throughout the world, projected in the range of 8%–12%. The second set of columns, labeled "Population", confirms that CC leads to a reallocation of the global population from developing to developed countries, as Europe, North America, and Oceania gain population. International migration caused by SO factors includes only voluntary migrants who seek economic prosperity subject to cross-border mobility constraints. However, even if South–North movements are dominant, population changes in developed and developing regions are rather small in scale, as global migration barriers tend to be hard to surmount. Moreover, this reallocation of workers has little effect on globally scaled population dynamics.

In the third set of columns, labeled "HS share", we analyze the impact of CC on the share of college graduates in the global labor force. These changes are negative in all continents, since emigrants from poor areas are positively selected along the skill dimension, but tend to be less educated than the native populations of the host areas. However, as the century progresses, this movement from poorer to richer regions and countries improves the access to education, which gradually leads to a greater global share of college graduates (an increase by 0.2% in 2070 and by 0.7% in 2100

TABLE 1. Aggregate effects of SO factors on the world economy (percentage changes).

Continent/		GDP			Population			HS share			Urbanization			Emigration shares		
Scenario		'40	'70	'00	'40	'70	'00	'40	'70	'00	'40	'70	'00	'40	'70	'00
AFR	RCP4.5	−9.0	−19.0	−22.5	−0.1	−0.2	−0.4	−0.3	−0.3	0.0	0.5	1.3	0.5	1.5	2.3	2.6
	RCP7.0	−10.1	−24.7	−34.9	−0.1	−0.3	−0.5	−0.3	−0.4	−0.1	0.6	1.8	1.0	1.7	3.1	4.2
	RCP8.5	−11.6	−29.9	−41.3	−0.1	−0.4	−0.7	−0.4	−0.5	−0.2	0.7	2.3	1.5	1.8	4.0	6.0
ASI	RCP4.5	−5.3	−11.7	−15.1	−0.1	−0.2	−0.4	−0.1	−0.1	−0.1	0.0	0.1	0.2	1.0	2.1	3.2
	RCP7.0	−5.5	−14.6	−22.0	−0.1	−0.3	−0.5	−0.1	−0.2	−0.2	0.0	0.2	0.4	0.9	2.7	4.7
	RCP8.5	−7.0	−19.0	−28.7	−0.1	−0.4	−0.7	−0.2	−0.3	−0.4	0.1	0.3	0.7	1.4	4.2	7.6
EUR	RCP4.5	1.2	2.7	3.7	0.5	1.6	2.6	−0.1	−0.4	−0.5	−0.2	−0.1	−0.1	−0.6	−1.8	−2.1
	RCP7.0	1.3	3.4	5.0	0.6	2.0	3.7	−0.1	−0.4	−0.8	−0.2	−0.1	0.0	−0.7	−2.5	−3.5
	RCP8.5	1.5	3.4	4.7	0.7	2.5	4.8	−0.1	−0.5	−1.0	−0.2	−0.1	0.1	−0.9	−3.0	−4.4
AMS	RCP4.5	−8.2	−15.0	−17.9	−0.4	−1.0	−1.5	0.0	−0.1	−0.3	0.2	0.3	0.5	3.1	5.4	5.9
	RCP7.0	−9.1	−19.9	−27.5	−0.4	−1.2	−2.2	0.0	−0.1	−0.3	0.2	0.4	0.8	3.4	7.5	10.4
	RCP8.5	−10.5	−24.3	−34.3	−0.5	−1.5	−2.8	0.0	−0.1	−0.3	0.2	0.5	1.0	3.9	9.4	13.7
AMN	RCP4.5	−2.4	−4.0	−4.3	0.6	1.5	2.1	−0.4	−0.6	−0.7	−0.1	−0.2	−0.2	−1.1	−1.6	−1.3
	RCP7.0	−2.9	−5.6	−7.8	0.6	1.8	2.8	−0.4	−0.8	−1.0	−0.1	−0.3	−0.3	−1.0	−2.3	−2.6
	RCP8.5	−3.0	−6.9	−10.2	0.8	2.5	3.8	−0.4	−1.0	−1.3	−0.1	−0.3	−0.4	−1.5	−3.2	−3.7
OCE	RCP4.5	−0.2	−0.8	−1.0	0.8	1.8	2.3	−0.5	−0.5	−0.6	−0.4	−0.8	−1.0	0.2	0.9	1.6
	RCP7.0	−0.6	−1.9	−3.0	0.8	2.0	2.9	−0.5	−0.8	−1.1	−0.5	−1.2	−1.8	0.3	1.4	2.8
	RCP8.5	−0.7	−2.3	−4.1	0.9	2.7	4.1	−0.6	−1.0	−1.6	−0.6	−1.5	−2.5	0.2	1.5	3.4
WLD	RCP4.5	−3.1	−6.1	−7.3	0.0	0.0	0.0	0.0	0.2	0.6	0.1	0.5	0.4	1.1	1.9	2.4
	RCP7.0	−3.4	−8.0	−11.8	0.0	0.0	0.0	0.0	0.2	0.7	0.1	0.7	0.8	1.1	2.5	3.7
	RCP8.5	−4.0	−10.2	−15.2	0.0	0.0	0.0	0.0	0.3	0.9	0.2	0.9	1.1	1.4	3.6	5.5

Notes: Table 1 summarizes the aggregated effects of SO CC scenarios as of 2040, 2070, and 2100 for Africa (AFR), Asia (ASI), Europe (EUR), South America (AMS), North America (AMN), Oceania (OCE), and the world (WLD). For each region, we present the outcomes as the *percentage changes* for RCP4.5, the benchmark RCP7.0, and RCP8.5. The highlighted macroeconomic variables considered are GDP in US dollars, the adult population aged 30–60 years, the share of HS adult workers, urbanization rate, and the share of adults migrating internationally. The percentage changes of these respective macroeconomic variables are computed relative to the RCP0.0 reference scenario, in which climate variables are kept constant at their 2010 levels throughout the 21st century.

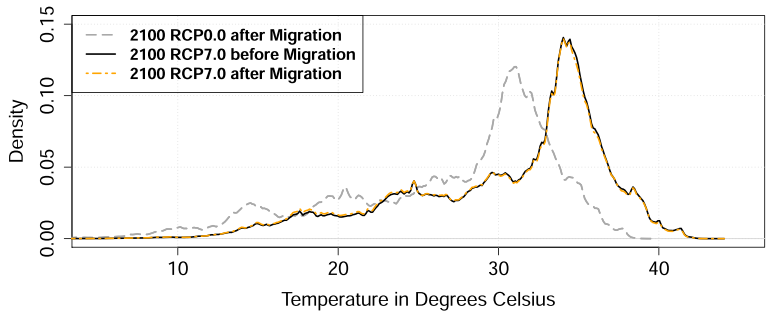

FIGURE 5. Population-weighted distribution of global temperature levels in 2100. This figure plots three distributions of global temperature levels weighted by pixel-specific populations for RCP0.0 (gray long-dashed line), and RCP7.0 in 2100: The black solid line includes the population distribution before migration, while the orange dot–dashed line considers the population after this migration occurs.

under RCP7.0). The fourth set of columns in Table 1 shows that CC accelerates urbanization in Africa, Asia, and South America, where the share of urban workers increases by up to 1% due to CC in RCP7.0 (Thiede, Gray, and Mueller 2016; Peri and Sasahara 2019; Castells-Quintana, Krause, and McDermott 2021). In the already-rich continents—North America, Europe, and Oceania—CC slows down urbanization because of negative productivity shocks in cities after the inflows of less-educated migrants. Finally, the last set of columns depicts changes in aggregated international emigration shares, showing that: (i) CC increases the global share of emigrants by 1–4 percentage points under RCP7.0 (ii) cross-border mobility serves as an important adaptation strategy to CC in some parts of the developing world, while under constant migration laws and policies, and (iii) the developed countries manage to discourage their citizens from migrating.

When focusing exclusively on SO factors, migration in general, and international migration in particular, plays a limited role in helping humans escape climate damage. Since under the SO scenario, all migration is voluntary, the number of migrants corresponds to small fractions of the total national and global populations, and does not induce a massive relocation across country borders. Figure 5 illustrates this fact with a population-weighted distribution of temperature computed for all pixels in the model. Obviously, due to CC, the distribution moves significantly to the right as, by definition, the planet heats up considerably under RCP7.0 compared with a no-CC base case (the latter depicted by the gray long-dashed line). However, the comparison of population distributions in 2100 under RCP7.0 before and after CC-induced mobility (black solid and orange dot–dashed lines, respectively) reveals only very small differences. In particular, one might spot tiny variations at the peak of the distributions (i.e. around 35°C), and close to 17°C–22°C. The movement from hotter to cooler areas is limited, showing that long-haul migration does not emerge as a first-order adaptation strategy when considering SO trends.

TABLE 2. Global numbers of climate migrants over the 21st century (in millions).

	Local				Regional				International			
Scenario	'40	'70	'00	∑	'40	'70	'00	∑	'40	'70	'00	∑
RCP4.5	−0.6	−1.9	−2.0	**−4.5**	−0.9	−2.4	−3.0	**−6.3**	2.5	4.8	5.7	**13.0**
RCP7.0	−0.7	−2.6	−3.3	**−6.6**	−0.9	−3.2	−4.8	**−8.9**	2.5	6.3	8.9	**17.7**
RCP8.5	−0.9	−3.5	−4.5	**−8.9**	−1.1	−3.9	−5.9	**−10.9**	3.2	8.9	13.5	**25.6**
RCP4.5 SLR	4.2	0.9	−0.1	**5.0**	6.1	1.1	0.9	**8.1**	7.8	7.1	8.0	**22.9**
RCP7.0 SLR	4.2	0.2	−1.0	**3.4**	6.1	0.5	−0.4	**6.1**	7.8	8.8	11.4	**28.0**
RCP8.5 SLR	4.0	−0.4	−1.8	**1.8**	5.9	0.2	−0.9	**5.2**	8.5	11.6	16.4	**36.5**
RCP4.5 SLRFO	3.7	−0.9	−3.0	**−0.3**	5.7	2.0	1.5	**9.3**	11.5	11.9	13.2	**36.6**
RCP7.0 SLRFO	3.7	−1.9	−6.1	**−4.3**	5.6	2.2	2.3	**10.1**	11.8	16.8	28.2	**56.8**
RCP8.5 SLRFO	3.4	−3.5	−10.0	**−10.2**	5.8	3.3	4.0	**13.1**	15.1	29.4	49.7	**94.1**

Notes: Table 2 shows the model's predicted changes in the aggregate number of migrants (in millions) for the RCP4.5, RCP7.0, and RCP8.5 scenarios, relative to the hypothetical RCP0.0 scenario, in which climate variables are kept constant over the 21st century and equal to the 2010 values. These changes are shown in 2040, 2070, and 2100. Numbers in bold are the sum of estimates over the simulation period. In the top panel, we only consider SO factors; in the middle panel, we consider changes caused by SO factors and rising sea levels; and in the bottom panel, we show the results from the most comprehensive model that combines changes caused by SO factors, rising sea levels, and FO factors.

4.2. Sea Level Rise

When we add in the second factor, rising sea levels that will result from global warming, coastal flooding is shown to generate millions of forcibly displaced people. According to our quantification in Section 2.2, 47 million people aged 30–60 years live in coastal areas that incur the risk of additional flooding during the 21st century under the RCP7.0 scenario. Table 2 presents the aggregated numbers of migrants by year and by migration type for three sets of results, namely SO in the top panel, SO and SLR jointly in the middle panel, and the combined SO, SLR, and FO factors in the bottom panel. (The third scenario will be discussed in the next section.) Unlike the SO only scenario, where international migration clearly acts as a substitute for internal (local and regional) movements, adding SLR translates into a greater number of people choosing all types of migration: local, regional, and international. The major impact of SLR is visible in short-distance moves, as this type of relocation is associated with smaller monetary, psychological, and information costs. International migration is affected by coastal flooding to a (relatively) lesser extent. Taking the difference between the middle and top panels of Table 2, 25%–30% of SLR-induced migrants choose to migrate internationally, while 40%–50% move interregionally within their home country.

Even though the direct pressure of SLR on international migration is limited, higher ocean levels have an important impact on the attractiveness of many seaboard areas. Coastal regions tend to be more densely populated, more productive, and more popular as destinations for migrants (either regional or international). With coastal flooding, some of these regions become inhabitable, which significantly changes the distribution

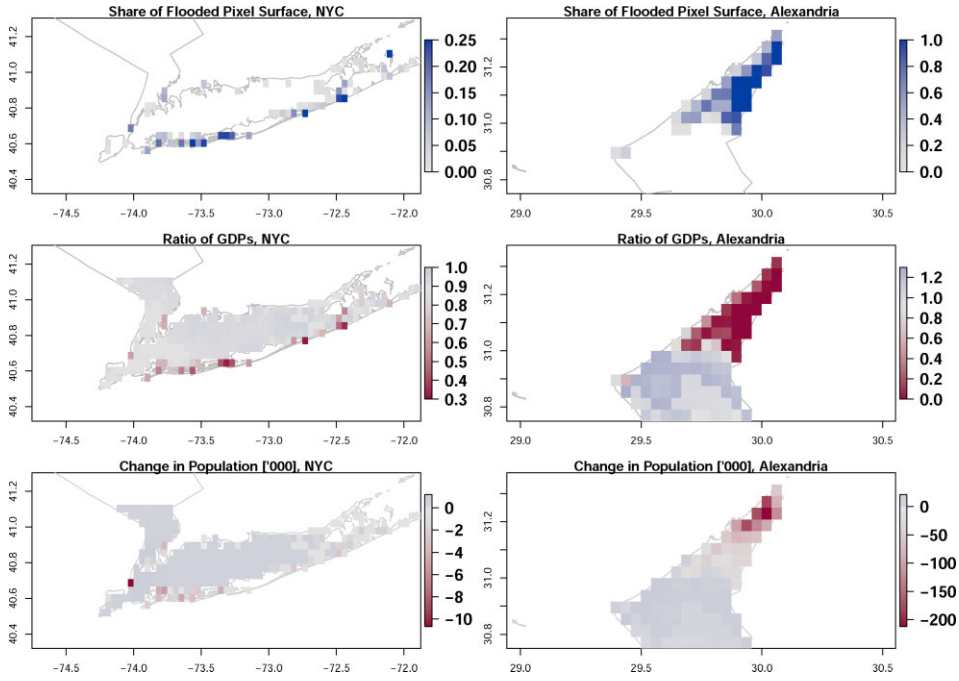

FIGURE 6. Rising sea levels and their impact on New York City, Long Island, and Alexandria in 2100. This figure depicts the spatial extent of SLR in New York City and Long Island (left panel) and the city of Alexandria, Egypt (right panel), in 2100 for RCP7.0. The top panels illustrate pixel-specific coastal flooding, the middle panels show ratios of pixel-specific GDP levels after/before flooding, while the bottom panels plot changes in population (in thousand people). All deviations are computed as differences between RCP7.0 with SLR and RCP7.0 without SLR.

of economic activity in specific localities highly exposed to SLR. In addition, SLR also boosts voluntary migration.[29] Let us take two examples to illustrate these indirect effects of SLR, New York City and Long Island in the United States (left panel), and the Egyptian city of Alexandria (right panel) in Figure 6. According to these maps, some densely populated and productive areas are economically wiped off the map and become depopulated. Crucially, pixels within these two urban areas that have not been entirely flooded are also negatively affected due to technological spillovers and partial TFP losses, which undermine local labor markets and discourage people from staying. Even though we see a strong local displacement of people to nearby areas, an important share of the flooded-out population leaves both regions. On the flip side, the expected utility of migrating to the New York State and to the Alexandria Governorate drops, as does the utility of the United States and Egypt as destinations for international migrants. In this way, the local damage caused by SLR contributes to transforming global mobility patterns.

29. Remember that we assume that each pixel q flooded to a degree $\varphi_t(q) \in (0, 1]$ in time t loses a share $\varphi_t(q)$ of its TFP. This discourages the non-flooded inhabitants of this pixel to stay.

4.3. Fast-Onset Factors

We now implement our preferred and most comprehensive specification that accounts for three concurrent types of CC shocks, namely SO, SLR, and FO factors. As discussed in Section 2.3, we add the calibrated expected utility and economic losses caused by natural disasters (droughts, floods, and storms) and heatwaves. Extreme weather events are spatially concentrated in specific territories, leaving certain regions more exposed to damage, as shown in Figure 4. Therefore, the economic impact of FO factors generates a substantial incentive to migrate. However, internal migration responses are somewhat limited due to the spatial correlation in FO shocks. In contrast, as shown in Table 2, the number of international migrants increases significantly, by a factor of 2–3. The remainder of this subsection decomposes these adjustments, highlighting the benefits from working with a high resolution data on CC shocks.

We start with presenting the continent-specific changes in key macroeconomic and demographic variables over the 21st century for the three RCP scenarios. Comparing RCP7.0 with the no-CC base case, Table 3 shows that global GDP falls by 4.5%, 9.3%, and 12.7% in 2040, 2070, and 2100, respectively. Relative to Table 1, the economic losses due to SLR and extreme events are roughly equal to 1 percentage point of GDP at the global scale. The spatial distribution of climate damage is strongly heterogeneous as African, South American, and Asian countries are severely affected by the combined SO, SLR, and FO shocks, with GDP losses of up to 30% and 40%, significantly more than in the case of SO. In contrast, Europe and (to a lesser extent) Oceania remain immune to CC-induced economic losses, mainly due to the influx of migrants (as evidenced by projected population changes). Importantly, while the share of HS workers drops in all regions (due to the positive selection in out-migration from poor regions (Drabo and Mbaye 2015), and the lower supply of human capital among climate immigrants relative to citizens of richer destinations), the overall number of highly educated workers increases at the global scale. However, this effect is smaller than in the SO simulation of Table 1 and only materializes in 2100. As expected, CC creates supportive conditions for people to relocate from rural to urban areas, and this phenomenon is accentuated by SLR and FO shocks. Similar to the findings in Peri and Sasahara (2019), Thiede, Gray, and Mueller (2016), and Castells-Quintana, Krause, and McDermott (2021), our model shows that urbanization rates increase by more than 2% in Africa and Asia by the late 21st century (twice the change obtained with SO factors only). More CC-induced damage translates into significantly more climate migrants originating from Africa, Asia, and South America, as mean emigration rates for these continents rise by over 10%. The phenomenon is perceptible at the world level as well. Alongside SO factors, SLR and FO shocks are instrumental to understanding how future CC is likely to govern interregional and international mobility.

Although Table 3 provides an aggregated view of CC's effect on economic prosperity and migration, the geographical distribution of the intensity of CC-related factors varies substantially across the globe. The first panel of Figure 7 depicts changes in GDP per capita in 2100 under the RCP7.0 scenario. The largest losses

TABLE 3. Aggregate effects of SO, SLR, and FO shocks on the world economy (percentage changes).

Continent/		GDP			Population			HS share			Urbanization			Emigration shares		
Scenario		'40	'70	'00	'40	'70	'00	'40	'70	'00	'40	'70	'00	'40	'70	'00
AFR	RCP4.5	−14.5	−25.7	−27.8	−0.3	−0.6	−0.9	−0.9	−1.0	−1.1	0.3	1.9	1.4	7.0	6.0	7.0
	RCP7.0	−14.9	−30.9	−40.1	−0.3	−0.7	−1.2	−1.0	−1.1	−1.0	0.4	2.6	2.4	7.5	9.3	14.9
	RCP8.5	−18.2	−39.2	−51.8	−0.4	−0.9	−1.7	−1.2	−1.5	−1.5	0.5	3.2	2.9	8.7	14.2	22.8
ASI	RCP4.5	−7.9	−15.7	−19.2	−0.2	−0.6	−1.2	−0.3	−3.1	−4.2	−0.4	−0.3	0.4	6.2	5.9	6.9
	RCP7.0	−7.8	−18.3	−25.8	−0.2	−0.7	−1.6	−0.3	−3.2	−4.5	−0.4	−0.1	1.2	6.2	7.9	15.2
	RCP8.5	−10.1	−23.8	−33.4	−0.3	−1.1	−2.4	−0.5	−3.7	−5.1	−0.3	0.4	2.5	8.5	15.7	30.8
EUR	RCP4.5	0.9	3.0	4.5	1.2	3.0	4.7	−0.4	−0.8	−1.2	−0.2	−0.1	0.1	−0.1	−1.7	−1.6
	RCP7.0	1.2	4.0	6.7	1.2	3.7	6.8	−0.4	−1.1	−1.9	−0.2	0.0	0.2	−0.3	−2.7	−3.8
	RCP8.5	1.4	4.8	8.1	1.5	5.2	10.3	−0.4	−1.4	−2.9	−0.2	0.1	0.3	−0.6	−3.9	−6.3
AMS	RCP4.5	−11.9	−20.4	−23.9	−0.7	−1.6	−2.3	−0.1	−0.4	−1.1	0.0	0.1	0.2	6.5	7.5	7.6
	RCP7.0	−12.3	−25.1	−34.0	−0.8	−1.9	−3.2	−0.1	−0.3	−1.1	0.1	0.2	0.5	6.9	10.3	13.4
	RCP8.5	−15.0	−32.4	−44.5	−0.9	−2.5	−4.6	−0.1	−0.3	−1.3	0.1	0.3	0.7	8.0	14.7	21.6
AMN	RCP4.5	−2.3	−3.6	−3.6	1.9	3.4	4.4	−0.7	−0.9	−0.9	−0.2	−0.3	−0.3	−2.2	−1.3	0.1
	RCP7.0	−2.7	−5.1	−7.0	1.9	4.0	5.8	−0.8	−1.2	−1.4	−0.2	−0.4	−0.5	−2.1	−2.2	−1.5
	RCP8.5	−2.6	−5.9	−8.4	2.5	5.9	9.4	−0.9	−1.7	−2.4	−0.3	−0.5	−0.7	−3.2	−3.9	−3.3
OCE	RCP4.5	0.8	−0.1	−0.7	3.2	5.1	6.1	−1.8	−1.5	−1.1	−1.0	−1.3	−1.3	−1.5	0.8	2.6
	RCP7.0	0.2	−1.2	−2.1	3.2	5.7	7.8	−2.0	−1.9	−2.1	−1.2	−1.8	−2.1	−1.3	1.1	3.2
	RCP8.5	0.6	−0.7	−2.9	3.9	8.0	11.6	−2.1	−2.5	−3.0	−1.2	−2.1	−2.8	−2.1	0.4	3.9
WLD	RCP4.5	−4.3	−7.6	−8.5	0.0	−0.1	−0.1	0.0	−0.5	−0.1	−0.1	0.6	1.1	5.1	4.8	5.6
	RCP7.0	−4.5	−9.3	−12.7	0.0	−0.1	−0.2	0.0	−0.5	0.2	−0.1	1.0	1.8	5.3	6.8	11.9
	RCP8.5	−5.3	−11.7	−16.2	0.0	−0.1	−0.2	0.0	−0.3	0.9	0.0	1.5	2.7	6.7	11.9	20.8

Notes: Table 3 summarizes the aggregated effects as of 2040, 2070, and 2100 for Africa (AFR), Asia (ASI), Europe (EUR), South America (AMS), North America (AMN), Oceania (OCE), and the world (WLD). For each region, we present the outcomes as the percentage changes for RCP4.5, the benchmark RCP7.0, and RCP8.5. The highlighted macroeconomic variables considered are GDP in US dollars, the adult population aged 30–60 years, the share of HS adult workers, urbanization rate, and the share of adults migrating internationally. The percentage changes of these respective macroeconomic variables are computed relative to the RCP0.0 reference scenario, in which climate variables are kept constant at their 2010 levels throughout the 21st century.

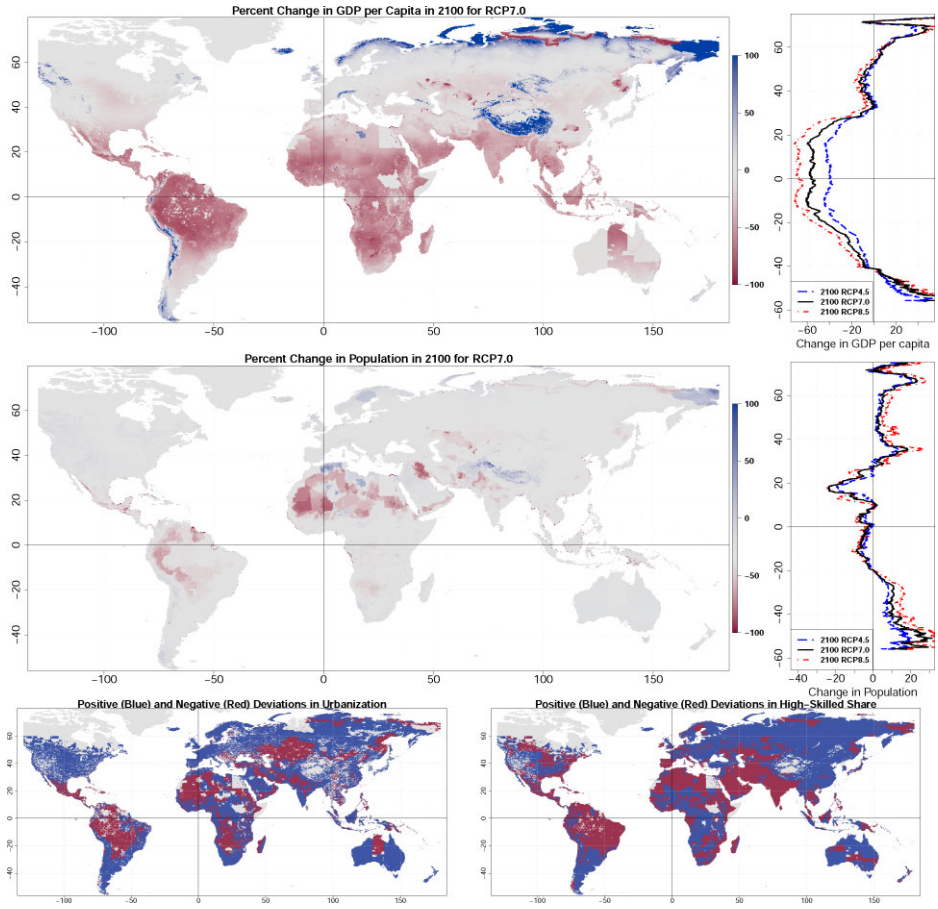

FIGURE 7. Changes in GDP per capita, population, urbanization, and the share of HS in 2100 under RCP7.0. This figure depicts the spatial distribution of changes in GDP per capita (top panels), population (middle panels), urbanization (bottom-left panel), and the share of HS adults (bottom-right panel) in 2100, due to SO, SLR, and FO shocks and under RCP7.0. All graphs illustrate deviations relative to the RCP0.0 reference, in which climate variables are kept constant at their 2010 levels throughout the 21st century. The top and middle panels depict changes in percent, while bottom panels show positive deviations (in blue) and negative deviations (in red).

are experienced in regions between the 20th parallels of the north and south latitudes, and are concentrated in relatively sparsely populated areas of Latin America and Central Africa, as well as highly populated regions in Southeast Asia and the Persian Gulf. Overall, the correlation between the magnitudes of climate damage and latitude remains strong, with losses visibly dependent on the particular RCP scenario (see the top-right panel of Figure 7). The least populated regions show the highest relative declines in population (see the middle panels of Figure 7). As expected, people tend to relocate from lower to higher latitudes, and the patterns of changes in relative population sizes are only moderately affected by the RCP scenarios (see the line graph

to the right in the middle panel). Only a few macroregions in the world experience significant increases in population, namely North Africa, the northern parts of India and Pakistan, and Siberia.

The bottom-left panel of Figure 7 presents the changes in urbanization across all pixels (measured as positive or negative deviations in urbanization rate). Deglomeration due to loss of population dominates in the severely affected regions, whereas a further concentration of urban populations prevails in destination areas for climate migrants, including areas of Africa, Asia, and coastal South America. When it comes to changes in the supply of skills, the bottom-right panel of Figure 7 confirms the patterns highlighted in the third set of columns of Table 3. On the one hand, regions exposed to CC lose relatively more HS workers, who face lower migration costs. On the other hand, in the richer and more developed countries, many urban destinations experience inflows of migrants from the poorer regions of the world. As climate movers are positively selected, the loss of human capital in the poorest areas, the ones most adversely regions affected by CC, accentuates the deepening of extreme poverty, an outcome discussed below. Consequently, both poor and rich areas lose human capital, and the shares of HS workers deteriorate in sending and receiving pixels (e.g. see India). Nevertheless, CC boosts the global supply of skills due to migration from less developed (less urbanized) areas to richer and more densely populated locales.

Looking in more detail at migration projections, we can highlight some interesting findings. Table 4 summarizes continent-specific changes in the stocks of migrants over the 21st century under the three RCP scenarios, decomposing the total numbers (the first set of columns) by the skill level of migrants (the second and third sets of columns), and by the type of migration (the last three sets of columns). First, the total number of CC-induced migration among adult workers (of all skills and all types) over the century equals 45 million under RCP4.5, 62 million under RCP7.0, and 97 million under RCP8.5.[30] Second, the continent-specific numbers of climate migrants vary across the RCP scenarios. Africa and Asia have the highest volatility relative to the various climate scenarios, and the response of these two continents fundamentally shapes the global aggregates. Third, approximately 15% of global movers are HS, although this share varies across continents. Asia is at the lower end of skilled migration share, while we find Africa and rich areas at the higher end. Positive selection in climate migration has implications for global inequality and extreme poverty. Fourth, the continents severely impacted by CC (Africa, Asia, and South America) experience negative deviations in local and regional mobility as spatial clustering of (especially extreme) climate shocks force displaced people to move over longer distances. Simultaneously, these areas see disproportionately large outflows of international migrants. Thus, as concluded for the analysis of SO factors, people tend to substitute local and regional migration options with cross-border destinations. Conversely, Europe, North America, and Oceania observe higher stocks of local and regional migrants due to CC, with little effects on international mobility. Overall, poor regions are expected to account

30. These numbers, multiplied by factor 2, would roughly correspond to migrants of all ages.

TABLE 4. Aggregate numbers of climate migrants over the 21st century.

Continent/		Total			Low skill			High skill			Local			Regional			International		
Scenario		’40	’70	’00	’40	’70	’00	’40	’70	’00	’40	’70	’00	’40	’70	’00	’40	’70	’00
AFR	RCP4.5	4.3	0.5	−0.6	3.8	−0.1	−1.3	0.5	0.6	0.7	1.0	−1.7	−3.6	0.6	−1.6	−2.7	2.6	3.9	5.7
	RCP7.0	4.3	1.2	2.2	3.7	0.5	1.1	0.5	0.7	1.1	1.0	−2.7	−6.6	0.5	−2.2	−3.9	2.8	6.1	12.7
	RCP8.5	4.5	2.7	6.3	3.9	1.9	5.0	0.6	0.8	1.3	0.9	−3.8	−8.7	0.3	−2.9	−4.4	3.3	9.4	19.4
ASI	RCP4.5	13.3	8.0	5.5	11.6	8.6	7.2	1.8	−0.6	−1.7	2.4	−0.4	−1.8	4.4	2.6	2.2	6.6	5.8	5.2
	RCP7.0	13.4	11.0	14.4	11.6	11.2	15.2	1.8	−0.2	−0.8	2.4	−0.4	−2.1	4.4	3.5	4.1	6.5	7.9	12.4
	RCP8.5	16.2	20.3	26.5	14.0	19.5	26.4	2.2	0.8	0.1	2.2	−1.1	−4.7	4.9	5.3	5.5	9.0	16.1	25.6
EUR	RCP4.5	0.7	1.3	2.2	0.5	1.0	1.6	0.2	0.3	0.6	0.1	0.6	0.9	0.2	0.3	0.4	0.4	0.4	0.9
	RCP7.0	0.7	1.2	2.3	0.5	1.0	1.7	0.2	0.3	0.6	0.1	0.6	1.0	0.2	0.3	0.5	0.3	0.3	0.8
	RCP8.5	0.7	1.3	2.8	0.5	1.1	2.2	0.2	0.3	0.6	0.1	0.7	1.2	0.2	0.3	0.7	0.3	0.4	1.0
AMS	RCP4.5	2.3	1.0	0.2	1.8	0.7	0.1	0.5	0.3	0.1	0.1	−0.2	−0.2	0.2	−0.4	−0.6	2.0	1.6	1.0
	RCP7.0	2.4	1.4	0.6	1.9	1.0	0.4	0.5	0.4	0.2	0.0	−0.3	−0.3	0.2	−0.7	−1.0	2.1	2.3	1.9
	RCP8.5	2.6	2.1	1.2	2.0	1.6	0.8	0.5	0.5	0.4	0.0	−0.3	−0.5	0.1	−0.9	−1.4	2.5	3.3	3.1
AMN	RCP4.5	0.3	1.2	2.4	0.2	0.5	1.0	0.1	0.7	1.3	0.1	0.3	0.6	0.2	0.8	1.5	0.0	0.1	0.2
	RCP7.0	0.3	1.3	2.7	0.2	0.6	1.2	0.1	0.7	1.5	0.1	0.3	0.7	0.2	0.9	1.8	0.0	0.1	0.2
	RCP8.5	0.3	1.6	3.8	0.2	0.8	1.9	0.1	0.8	1.9	0.1	0.4	1.0	0.2	1.1	2.5	0.0	0.1	0.3
OCE	RCP4.5	0.1	0.9	1.9	0.1	0.7	1.4	0.0	0.3	0.5	0.0	0.5	1.1	0.0	0.4	0.7	0.0	0.1	0.2
	RCP7.0	0.1	1.0	2.2	0.1	0.7	1.6	0.0	0.3	0.6	0.0	0.5	1.2	0.1	0.4	0.8	0.0	0.1	0.2
	RCP8.5	0.1	1.2	3.0	0.1	0.9	2.2	0.0	0.3	0.8	0.0	0.6	1.7	0.1	0.5	1.1	0.0	0.1	0.3
WLD	RCP4.5	20.9	13.0	11.6	17.8	11.5	10.1	3.1	1.5	1.6	3.7	−0.9	−3.0	5.7	2.0	1.5	11.5	11.9	13.2
	RCP7.0	21.1	17.1	24.4	17.9	15.0	21.3	3.2	2.1	3.2	3.7	−1.9	−6.1	5.6	2.2	2.3	11.8	16.8	28.2
	RCP8.5	24.2	29.2	43.6	20.6	25.8	38.5	3.6	3.4	5.1	3.4	−3.5	−10.0	5.8	3.3	4.0	15.1	29.4	49.7

Notes: Table 4 illustrates changes in the number of migrants (in millions) who relocate because of factors related to CC as of 2040, 2070, and 2100 under the RCP4.5, RCP7.0, and RCP8.5 scenarios. Aggregate numbers are given for Africa (AFR), Asia (ASI), Europe (EUR), South America (AMS), North America (AMN), Oceania (OCE), and the world (WLD). From left to right, the first column reports the total number of migrants, then the number of LS migrants, followed by HS migrants, local migrants of all skill levels, regional migrants of all skill levels, and international migrants of all skill levels. The changes are computed relative to the RCP0.0 reference scenario, in which climate variables are kept constant at their 2010 levels throughout the 21st century.

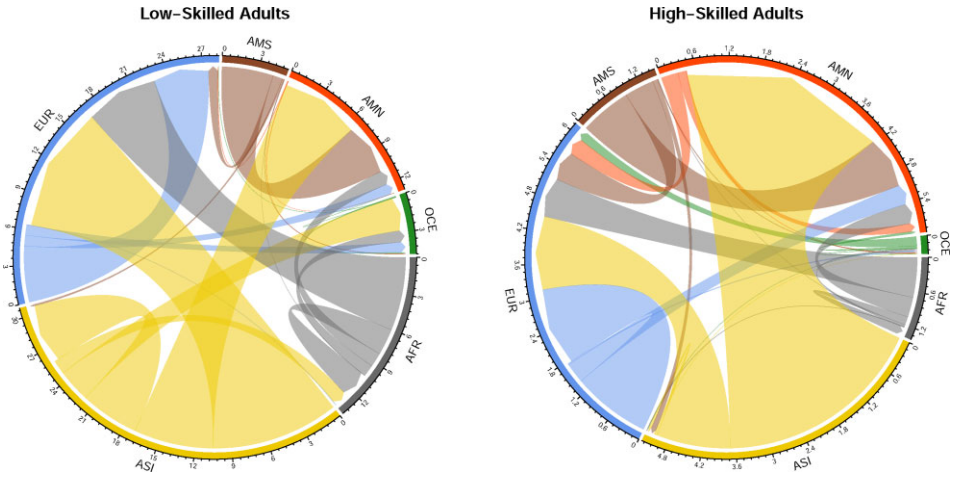

FIGURE 8. Climate-induced international migration paths. This figure depicts the projected stocks of international migrants responding to SO, SLR, and FO shocks. The charts present the sum of migrants in 2040, 2070, and 2100 under RCP7.0. The left (right) panel illustrates the total number of LS (HS) movers (expressed in millions of people) across six continents: Africa (AFR), Asia (ASI), Europe (EUR), South America (AMS), North America (AMN), and Oceania (OCE).

for an important amount of the total CC-induced international migrants over the course of 21st century. To recapitulate, in the RCP7.0 scenario, almost 22 million out of 57 million of cross-border movers originate from Africa, 27 million from Asia, and 6 million from South America. The migration crises generated by CC is mainly a story of South–North migration. However, considering the total projected populations aged 30–60 in these areas (1.5 billion in Africa, 1.6 billion in Asia, and 200 million in South America), not many citizens from the most damaged countries decide to move internationally. From our projections, it becomes clear that long-haul migration is a potential adaptation strategy to CC only for a minor share of the populations most at risk of suffering the negative effects of global warming.

However, climate migration from the world's developing regions can be an important policy topic from the perspective of the likely destination countries. Figure 8 illustrates the main directions of international mobility generated by CC under RCP7.0 at a continent-level granularity over the remainder of this century. Focusing exclusively on the LS (left panel), we observe four main paths of global population moves: from Asia to Europe (10 million people), from Asia to North America (6 million people), from Africa to Europe (6 million people), and from South America to North America (5.5 million people). These dyadic patterns roughly correspond to contemporary origin-destination pairs, but represent significantly larger sizes, which might induce social tensions in the wealthier countries, as many of these people could be perceived as economic (voluntary) migrants, not forcibly displaced victims of CC. In some destination countries, a climate migration crisis can become a source of political tension. Simultaneously, the HS international migrants who decide to move because

of CC are less numerous, but reveal more scattered patterns of mobility. The right panel of Figure 8 portrays a global picture with a predominant pathways from Asia to North America (3.6 million people), from Asia to Europe (1.5 million people), and from South America to North America (1 million people). Even though HS workers are more welcomed as immigrants in the richer parts of the world, they still encounter huge moving costs. Overall, our model does not predict massive numbers of international climate migrants.

Some places are particularly exposed to emigration and immigration shocks. Figure 9 presents the spatial distribution of gross stocks of emigrants and immigrants by education level over the 21st century. Focusing on the two left panels (illustrating LS movers), we can detect extensive areas of Central India, the Middle East, Mexico, and the northern part of sub-Saharan Africa where out-migration intensifies significantly due to CC over the 21st century. More developed areas, such as Europe, the United States, and Southeast Asia, are also subject to the increased mobility of less educated workers, as the productivity shocks and coastal flooding depress the economic potential of certain areas. Interestingly, some localities experience reduced mobility pressures (e.g. coastal India, scattered urban regions in Central Africa, and Central China). These are the developing regions, which benefit from incoming of CC-induced movers. Indeed, the bottom-left panel of Figure 9 explicitly indicates that the low-emigration pixels are predominantly located in the high-immigration areas. Only a few areas do not follow this polarized pattern, but instead experience a high-emigration and high-immigration pattern: coastal China, Southeast Asia, Israel, and Western Europe. In these areas, inflows of climate migrants encourage native citizens to relocate to suburbs, dissipating the initial immigration shock onto a broader territory.

When it comes to highly educated workers (right panels of Figure 9), the spatial patterns of out- and in-mobility are similar, although these movements are smaller by an order of magnitude. One can observe significant outflows of HS individuals from many coastal areas damaged by the SLR, for example, Eastern China, Japan, Western Europe, the coastal areas near the Bay of Guyana, and US Eastern Seaboard. Other skill-intensive regions are negatively affected by SO and FO factors, such as Iraq, the Middle East, the Nile Delta, Central India, North Latin America, and California. These outflows are mainly directed to urban areas that are relatively less affected by CC. For example, the cities of Mumbai and Kochi in the west coast of India, multiple coastal urban centers in China, the African coast between Accra (Ghana) and Douala (Cameroon), cities in Central Europe, the United Kingdom, and Russia, cities of Salvador, Rio de Janeiro, Sao Paulo, Porto Alegre, and Buenos Aires in South America, as well as US cities: those located in the northern part of the country between Chicago and Boston, and Seattle. The acceleration of urbanization around the world accentuates the further polarization of economic activity between cities and rural areas. This shift foments increasing inequality and generates even more concentrated and potentially overpopulated localities.

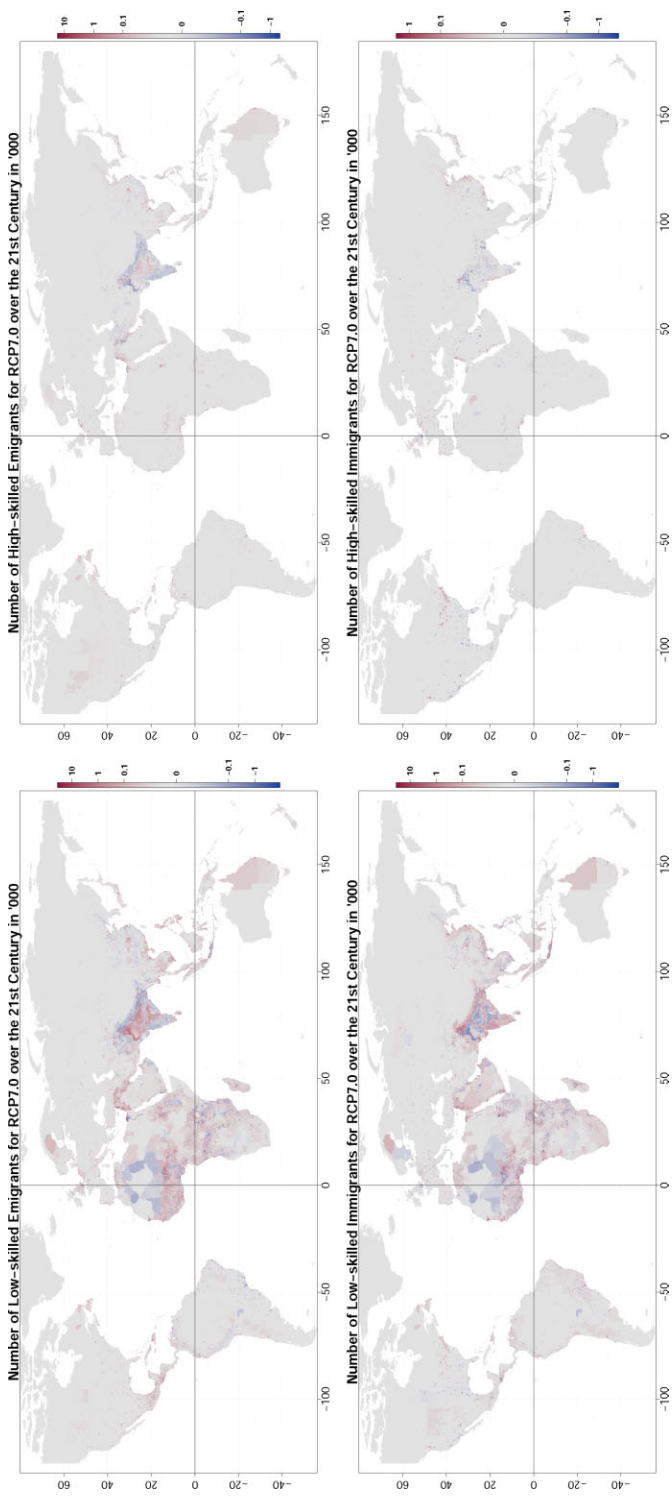

FIGURE 9. Variations in emigration and immigration over the 21st century, RCP7.0 versus RCP0.0. The maps illustrate pixel-specific distributions of gross numbers of LS/HS emigrants/immigrants for RCP7.0 SO, SLR, and FO, over the 21st century. All values are in thousands of people and computed relative to the RCP0.0 reference scenario, in which climate variables are kept constant at their 2010 levels throughout the 21st century.

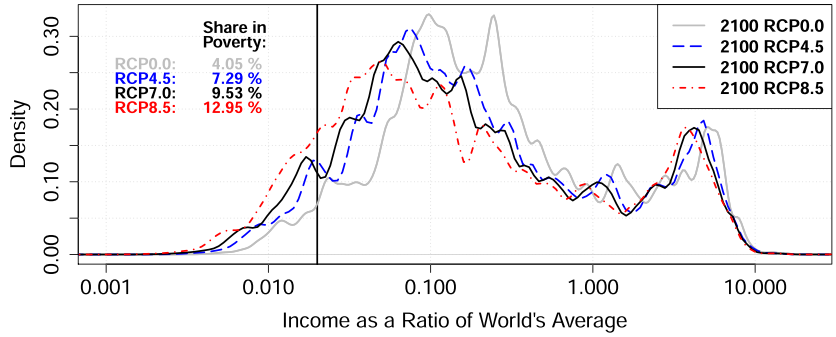

FIGURE 10. Population-weighted distributions of income in 2100. This figure illustrates the changes in relative distributions of income in 2100 for four emission scenarios: RCP0.0, in which climate variables are kept constant at their 2010 levels throughout the 21st century, RCP4.5, RCP7.0, and RCP8.5, including SO, SLR, and FO shocks. Income distributions are standardized to global average, and the horizontal axis is logarithmic. The vertical black line represents the UN relative poverty threshold set at 2% of the worldwide average level of income.

5. Policy Implications

CC materializes as a threat to global prosperity, regional cohesion, and livability in a large number of areas. A crude way to grasp the magnitude of the adverse effects on the world economy and quality of life is to visualize the impact that global warming will have on the world distribution of income (Benveniste et al. 2021). Figure 10 compares simulated income distributions for the year 2100 under four RCP scenarios with SO, SLR, and FO factors.[31] These distributions are normalized by the worldwide average level of income (i.e. a value of 1 is meant to represent the average level), and the horizontal axis is in a logarithmic scale. The black vertical line represents the relative poverty line defined by the UN at the level of 2% of worldwide average level of income.

The adverse implications of CC for individual prosperity around the world emerge clearly when comparing the four curves. The more severe the emission scenario, the more dominated is the distribution of income, which reflects the fact that billions of people suffer CC-driven income losses. Moreover, CC is to blame for a significant rise in extreme poverty. Without CC, 4.0% of the worldwide population will be under the 2% poverty line, whereas the population share in extreme poverty reaches 9.5% under RCP7.0, and 13.0% under RCP8.5. This roughly corresponds to 160 million adults in RCP0.0, 380 million in RCP7.0, and 520 million in RCP8.5. Importantly, even under the optimistic RCP4.5 scenario, an additional 140 million people will end up in extreme poverty. These are striking numbers that should motivate policymakers and other citizens to behave proactively in trying to mitigate the grim scenarios of significant global warming. Our analysis reveals that only a small fraction of these

31. Remember that RCP0.0 stands for the hypothetical no-CC scenario.

TABLE 5. Global numbers of climate migrants over the 21st century.

	Local				Regional				International			
Scenario	'40	'70	'00	∑	'40	'70	'00	∑	'40	'70	'00	∑
RCP4.5 SLRFO	3.7	−0.9	−3.0	**−0.3**	5.7	2.0	1.5	**9.3**	11.5	11.9	13.2	**36.6**
RCP7.0 SLRFO	3.7	−1.9	−6.1	**−4.3**	5.6	2.2	2.3	**10.1**	11.8	16.8	28.2	**56.8**
RCP8.5 SLRFO	3.4	−3.5	−10.0	**−10.2**	5.8	3.3	4.0	**13.1**	15.1	29.4	49.7	**94.1**
RCP7.0 MOB	2.7	−3.5	−10.4	**−11.2**	3.8	0.5	−3.5	**0.8**	14.3	23.1	39.4	**76.8**
RCP7.0 CAB	6.7	2.8	5.0	**14.5**	10.3	8.0	13.5	**31.9**	0.0	0.0	0.0	**0.0**
RCP7.0 CON	4.2	−0.5	−4.0	**−0.2**	7.6	5.7	6.7	**20.1**	16.4	20.7	31.4	**68.5**
RCP8.5 MOB&CON	0.5	−7.7	−15.0	**−22.2**	1.3	−2.6	−5.6	**−6.9**	14.9	35.1	61.7	**111.6**

Notes: Table 5 presents changes in the aggregated number of migrants (in millions of people) for given RCP scenarios. Note that the reference for all SO+SLR+FO scenarios and the CON scenario is RCP0.0, whereas references for migration policy scenarios MOB, CAB, and MOG & CAB are RCP0.0 MOB, RCP0.0 CAB, and RCP0.0 MOB, respectively. Numbers in bold are the sum of estimates over the simulation period.

CC-induced casualties will manage to move internally or internationally. This result implies that many people will be trapped in impoverished and troubled regions; hence, climate-induced poverty is likely to become the real threat to all of us. We next assess the consequences of alternative migration laws and policies that could be implemented to reduce the poverty that will likely increase due to CC. We also consider more uncertain scenarios involving conflicts over scarce resources in countries with the highest shortages in agricultural goods.

5.1. More Open Borders

One of the reasons why CC increases extreme poverty is that moving from low- to high-latitude countries requires crossing several borders and incurring large migration costs. International travel is particularly expensive for many people who aspire to migrate to richer regions in North America, Europe, and Oceania but originate from remote or rural developing areas. This is due to both legal migration barriers and large private relocation costs, as shown in Delogu, Docquier, and Machado (2018). We simulate here the consequences of a hypothetical easing of cross-border mobility barriers, labeling this scenario as More Open Borders (MOB). Starting from the middle-of-the-road base case (i.e. RCP7.0 with SO, SLR, and FO), the MOB variant implements a reduction in international migration costs in such a way that $(1 - x^i(n, n'))$ increases twofold across all country pairs, for all skill groups from 2040 onward. From equation (15), this means that the ratio of international migrants to stayers would double, all other things being equal.[32] We assess the impact of MOB on the number of climate migrants and the share of people in extreme poverty.

The row labeled "RCP7.0 MOB" in Table 5 provides the aggregate numbers of climate migrants by migration type and period after relaxing international migration

32. However, the actual impact on migration is a function of wage rates and congestion costs, all determined in the new general equilibrium.

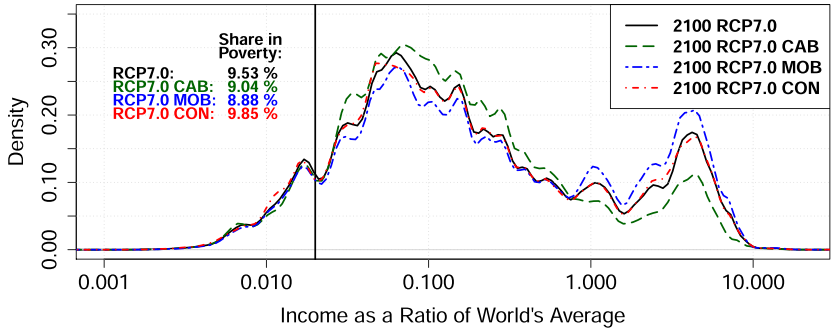

FIGURE 11. Population-weighted distributions of income in 2100. This figure illustrates the changes in relative distributions of income in 2100 for four RCP7.0-based scenarios: joint SO, SLR, and FO, a MOB scenario, a Closing All Borders (CAB) scenario, and a Conflict (CON) scenario. Income distributions are standardized to global average, the horizontal axis is logarithmic. The vertical black line represents the UN relative poverty threshold set at 2% of global average income.

barriers. Note that since this policy also affects economic migrants, our reference point is a hypothetical scenario of RCP0.0 MOB, in order to neutralize this policy impact on non-climate migration. While cross-border mobility due to CC rises visibly, local and regional movements plunge as people substitute short-distance mobility for long-haul movements. Over the entire 21st century, the stock of international climate migrants increases from 56.8 million in the RCP7.0 case to 76.8 million under the MOB variant, inducing greater immigration "pressures" in the high-income receiving countries.

However, the effects on global inequality and extreme poverty are mixed. The blue double-dashed curve in Figure 11 shows the world income distribution in the year 2100 under the MOB variant; it can be compared with the base case distribution in black solid line. Relaxing immigration barriers improves the global distribution of income and reduces the share of people mired in extreme poverty. As people are encouraged to move from poorer to richer regions, MOB involves a smaller share of the world population with income levels between 2% and 90% of the worldwide average, and a significantly greater share above 90%. However, despite large migration responses, the global share of extremely poor inhabitants falls to 8.9%, which is only 0.6 percentage point reduction of the result obtained under current migration policies. This finding suggests that a uniform increase in the net gain from international migration mostly benefits middle-income countries and slightly affects people trapped in the regions of the world most adversely impacted by CC. In this context, reducing carbon emissions seems a more effective policy option to lower the plight of those most vulnerable to climate poverty, as illustrated by the extreme poverty level obtained under the RCP4.5 scenario in Figure 10.

5.2. Closing All Borders

Another potential reason why CC increases extreme poverty is that climate migrants are positively selected along the skill dimension. The human capital flight from low-latitude countries can exacerbate the income loss incurred by the LS individuals left behind, as discussed in Benveniste, Oppenheimer, and Fleurbaey (2020) and McLeman (2019). As opposed to the first policy measure, we now consider a complete closure of international borders across all country pairs, for all skill groups, onward from 2040. This scenario is labeled CAB. This policy not only applies to climate migrants, but also affects migrants under the RCP0.0 scenario in the absence of CC. Thus, in Table 5, we present results comparing climate migration only by taking a hypothetical RCP0.0 CAB scenario as a reference. Row "RCP7.0 CAB" in Table 5 shows that 56.8 million of international CC-induced migrants are repatriated to their home countries under the CAB variant. Only approximately 40 million of them would relocate internally, which reflects the imperfect substitution between long-distance movements for short mobility. This means that more than 15 million would-be climate migrants are prevented or discouraged from escaping climate-related damage.

The distributional consequences of international border closures are depicted in Figure 11. The green long-dashed curve shows the world income distribution under the CAB variant, which can be compared with the base case scenario (RCP7.0 with SO, SLR, and FO). Unsurprisingly, closing international borders reduces the share of the world population living in high-income countries and increases the share living in middle- and low-income regions. Despite the magnitude of the shock, the share of the extremely poor drops to approximately 9%, only 0.5 percentage points below the share obtained in the base case scenario. Hence, stopping the brain drain makes the world poorer, but is of little help in fighting climate poverty.

5.3. Conflicts over Scarce Resources

Poverty, loss of livelihoods, and more difficult access to basic goods generate a fertile ground for conflicts. Gleditsch (2012), Burke, Hsiang, and Miguel (2015b), Carleton, Hsiang, and Burke (2016), and Abel et al. (2019) analyze the relationship between CC and conflicts over scarce resources. They find that extreme weather shocks increase the probability of armed conflicts and result in increased numbers of asylum seekers. An extensive body of research focuses on the impact of conflicts on economic prosperity and growth. This literature reports that wars have a sizable impact on economies, estimating the GDP loss in the range of 10%–33% (Collier 1999; Gleditsch et al. 2002; Abadie and Gardeazabal 2003; Murdoch and Sandler 2004; Blattman and Miguel 2010; Skaperdas 2011; Bove, Elia, and Smith 2017; Costalli, Moretti, and Pischedda 2017). In our quantification, we assume that CC-induced conflicts take place in those countries in which prices of agricultural goods rise by more than 10%, relative to a no-CC scenario. We also assume that given the conflict, the drop in income through productivity loss is uniform across all citizens in affected countries. For illustrative

purpose, this loss amounts to 20% in the top-10 afflicted countries, and 10% in countries placed in positions 11–20.[33] This exploratory conflict scenario is labeled CON.

According to the row "RCP7.0 CON" in Table 5, conflicts in countries strongly affected by CC generate additional 25 million climate migrants of all types over the 21st century, which is approximately 40% more than under the RCP7.0 scenario with SO, SLR, and FO factors. About half of them (i.e. 12 million people) choose international migration. Interestingly, these changes in global movements are smaller than the numbers obtained under the RCP8.5 scenario without conflicts (see Table 2). In its most pessimistic variant, CC itself is capable of generating significantly more migrants, confirming the conclusion that reducing emissions is the most efficient way of saving millions of people from climate-induced conflicts and climate-related damage. Similarly, conflicts push more people into misery, with 9.85% of the world population below the UN extreme poverty line. The poverty response to conflicts is smaller than the impact of RCP8.5 (almost 13% according to Figure 10). In the CON scenario, the overall distribution of global income changes visibly only below 10% of the world's average income, leaving the majority of the global population, though living in wealthier countries, unaffected by the scarcity of agricultural goods.

In the last line of Table 5, we present the aggregate stocks of migrants generated by the most pessimistic climate scenario, including RCP8.5 SO, SLR, and FO, extended by the combined MOB and CON scenarios. In this case, the superposition of multiple factors that reinforce international migrations causes the total numbers of movers to rise to 111 million over the 21st century. Even though the probability of realization of such an extreme scenario is low, it shows that the problem of global movements of people who want to avoid climate damage can easily get out of control.

6. Conclusion

The last decade has been the warmest on record, which indicates that global CC has already produced observable effects on the environment. These changes, however, are advancing at an unprecedented pace. In the summer of 2021, many areas of the Planet experienced catastrophic natural disasters, while July was the hottest month ever recorded. According to most climatologists, the process of CC is likely to accelerate even more during the remainder of this century and beyond, unless we succeed in a fast and drastic reduction of greenhouse gases emissions. The resulting damage will affect all countries and regions in a heterogeneous way, making many areas less attractive, less productive, or even inhabitable. In this paper, we use a structural approach to project the effect of predicted temperature trends, SLR, and damage due to natural

33. We consider the RCP7.0 with the SO, SLR, and FO scenario, and select 20 countries with highest increases in food prices (ordered from the highest increases in prices of agricultural goods): MDV, SUR, GMB, MRT, SEN, MLI, LBR, BFA, GIN, GHA, COG, VEN, SLE, CIV, BEN, KHM, AGO, TGO, SLV, and COD.

disasters for the world economy at a fine spatial resolution. Our micro-founded model translates official RCPs into projections of income distributions, differences in living standards, and a rise in extreme poverty. We confirm a well-established finding that low-latitude rural regions will be the most adversely affected, implying that CC is expected to reinforce inequality of opportunity across the globe. Going a step further, the main novelty of our approach comes from shedding light on the link between CC and migration patterns across millions of spatial cells over the course of the 21st century. Our micro-founded migration technology is consistent with current mobility data, and accounts for the interplay between alternative forms of migration, namely internal (local and regional) and international movements.

Assuming constant migration laws and policies, we predict that CC will increase the number of working-age migrants of all types by 45–97 million over the remainder of the 21st century. Adding dependent children, this means an approximate total of 100–200 million climate migrants. Under the middle-of-the-road RCP7.0 scenario, we predict 62 million climate migrants aged 30–60. These include 57 million international migrants, who mostly originate from sub-Saharan Africa, Asia, and South America. The aggregate numbers of international migrants are relatively small from the point of view of the sending countries, indicating that international climate migration will be a costly and perhaps unlikely adaptation strategy for the majority of people most affected by global warming. From the point of view of high-income receiving countries, these numbers are non-negligible but have limited effects on immigration rates compared with the effect of growing disparities in population growth. We conclude that massive international flows of migrants induced by climatic shocks are unlikely, except under a combined scenario that would include persistent conflicts over scarce resources, a wider opening of international borders, and the most pessimistic realization of the RCP8.5 pathway. Moderate migration responses to CC imply that many will be trapped in impoverished and troubled regions, inducing significant increases in extreme poverty. Although a gloomy vision of mass climate migration is frequently conveyed in the media and political sphere, we rather conclude that climate poverty is the real threat to all of us.

Appropriate policy responses are desirable to limit the effect of CC on global inequality and extreme poverty. We find that a uniform decrease in migration costs (stimulating migration across all pairs of countries and for all skill groups) or a strengthening of international migration barriers (reducing the brain drain) induces limited effects on climate poverty. Generous programs of development aid have also proved to be rather ineffective for decades, as aid involves scope for corruption or waste. Given the high sensitivity of extreme poverty rates to more adverse global warming scenarios, there is no better policy option than reducing emissions to limit climate poverty, inequality of opportunity, and pressures on healthcare systems.

References

Abadie, Alberto and Javier Gardeazabal (2003). "The Economic Costs of Conflict: A Case Study of the Basque Country." *American Economic Review*, 93(1), 113–132.

Abel, Guy J., Michael Brottrager, Jesus Crespo Cuaresma, and Raya Muttarak (2019). "Climate, Conflict and Forced Migration." *Global Environmental Change*, 54, 239–249.

Acemoglu, Daron (2002). "Technical Change, Inequality, and the Labor Market." *Journal of Economic Literature*, 40, 7–72.

Autor, David H., Frank Levy, and Richard J. Murnane (2003). "The Skill Content of Recent Technological Change: An Empirical Exploration." *The Quarterly Journal of Economics*, 118, 1279–1333.

Backhaus, Andreas, Inmaculada Martinez-Zarzoso, and Chris Muris (2015). "Do Climate Variations Explain Bilateral Migration? A Gravity Model Analysis." *IZA Journal of Migration*, 4, 3.

Barrios, Salvador, Luisito Bertinelli, and Eric Strobl (2006). "Climatic Change and Rural–Urban Migration: The Case of Sub-Saharan Africa." *Journal of Urban Economics*, 60, 357–371.

Barro, Robert J. and Jong Wha Lee (2013). "A New Data Set of Educational Attainment in the World, 1950–2010." *Journal of Development Economics*, 104, 184–198.

Bazzi, Samuel (2017). "Wealth Heterogeneity and the Income Elasticity of Migration." *American Economic Journal: Applied Economics*, 9, 219–55.

Beine, Michel and Christopher Parsons (2015). "Climatic Factors as Determinants of International Migration." *The Scandinavian Journal of Economics*, 117, 723–767.

Beine, Michel and Lionel Jeusette (2021). "A Meta-Analysis of the Literature on Climate Change and Migration." *Journal of Demographic Economics*, 87, 293–344.

Benveniste, Hélène, Jesús Crespo Cuaresma, Matthew Gidden, and Raya Muttarak (2021). "Tracing International Migration in Projections of Income and Inequality Across the Shared Socioeconomic Pathways." *Climatic Change*, 166, 1–22.

Benveniste, Hélène, Michael Oppenheimer, and Marc Fleurbaey (2020). "Effect of Border Policy on Exposure and Vulnerability to Climate Change." *Proceedings of the National Academy of Sciences*, 117, 26692–26702.

Berlemann, Michael and Max Friedrich Steinhardt (2017). "Climate Change, Natural Disasters, and Migration–A Survey of the Empirical Evidence." *CESifo Economic Studies*, 63, 353–385.

Berry, PAM, R. Smith, and J. Benveniste (2019). *Altimeter Corrected Elevations, Version 2 (ACE2)*. NASA Socioeconomic Data and Applications Center (SEDAC), Palisades, NY.

Bertoli, Simone and Jesús Fernández-Huertas Moraga (2013). "Multilateral Resistance to Migration." *Journal of Development Economics*, 102, 79–100.

Bindi, M., S. Brown, I. Camilloni, A. Diedhiou, R. Djalante, K. Ebi, F. Engelbrecht, J. Guiot, Y. Hijioka S. Mehrotra, et al. (2018). *Impacts of 1.5 °C of Global Warming on Natural and Human Systems*. IPCC, Geneva.

Black, Richard, Nigel W. Arnell, W. Neil Adger, David Thomas, and Andrew Geddes (2013). "Migration, Immobility and Displacement Outcomes Following Extreme Events." *Environmental Science & Policy*, 27, S32–S43.

Black, Richard, Stephen R. G. Bennett, Sandy M. Thomas, and John R. Beddington (2011). "Climate Change: Migration as Adaptation." *Nature*, 478, 447.

Blattman, Christopher and Edward Miguel (2010). "Civil War." *Journal of Economic Literature*, 48, 3–57.

Boas, Ingrid, Carol Farbotko, Helen Adams, Harald Sterly, Simon Bush, Kees van der Geest, Hanne Wiegel, Hasan Ashraf, Andrew Baldwin Giovanni Bettini, et al. (2019). "Climate Migration Myths." *Nature Climate Change*, 9, 901–903.

Borderon, Marion, Patrick Sakdapolrak, Raya Muttarak, Endale Kebede, Raffaella Pagogna, and Eva Sporer (2019). "Migration Influenced by Environmental Change in Africa." *Demographic Research*, 41, 491–544.

Bove, Vincenzo, Leandro Elia, and Ron P. Smith (2017). "On the Heterogeneous Consequences of Civil War." *Oxford Economic Papers*, 69, 550–568.

Burke, Marshall, John Dykema, David B. Lobell, Edward Miguel, and Shanker Satyanath (2015a). "Incorporating Climate Uncertainty into Estimates of Climate Change Impacts." *Review of Economics and Statistics*, 97, 461–471.

Burke, Marshall, Solomon M. Hsiang, and Edward Miguel (2015b). "Climate and Conflict." *Annual Review of Economics*, 7, 577–617.

Burzyński, Michal, Christoph Deuster, and Frédéric Docquier (2020). "Geography of Skills and Global Inequality." *Journal of Development Economics*, 142, 102333.

Cai, Ruohong, Shuaizhang Feng, Michael Oppenheimer, and Mariola Pytlikova (2016). "Climate Variability and International Migration: The Importance of the Agricultural Linkage." *Journal of Environmental Economics and Management*, 79, 135–151.

Carleton, T., Solomon M. Hsiang, and Marshall Burke (2016). "Conflict in a Changing Climate." *The European Physical Journal Special Topics*, 225, 489–511.

Carleton, Tamma A. and Solomon M. Hsiang (2016). "Social and Economic Impacts of Climate." *Science*, 353, aad9837.

Carter, Colin, Xiaomeng Cui, Dalia Ghanem, and Pierre Mérel (2018). "Identifying the Economic Impacts of Climate Change on Agriculture." *Annual Review of Resource Economics*, 10, 361–380.

Castells-Quintana, David, Melanie Krause, and Thomas K. J. McDermott (2021). "The Urbanising Force of Global Warming: The Role of Climate Change in the Spatial Distribution of Population." *Journal of Economic Geography*, 21, 531–556.

Cattaneo, Cristina, Michel Beine, Christiane J. Fröhlich, Dominic Kniveton, Inmaculada Martinez-Zarzoso, Marina Mastrorillo, Katrin Millock, Etienne Piguet, and Benjamin Schraven (2019). "Human Migration in the Era of Climate Change." *Review of Environmental Economics and Policy*, 13, 189–206.

Cattaneo, Cristina and Giovanni Peri (2016). "The Migration Response to Increasing Temperatures." *Journal of Development Economics*, 122, 127–146.

Church, John A., Peter U. Clark, Anny Cazenave, Jonathan M. Gregory, Svetlana Jevrejeva, Anders Levermann, Mark A. Merrifield, Glenn A. Milne, R. Steven Nerem Patrick D. Nunn, et al. (2013). "Sea Level Change." In *Climate Change 2013: The Physical Science Basis. Contribution of Working Group I to the Fifth Assessment Report of the Intergovernmental Panel on Climate Change*, edited by T. F. Stocker, D. Qin, G.-K. Plattner, M. Tignor, S. K. Allen, J. Boschung, A. Nauels, Y. Xia, V. Bex, and P. M. Midgley. Cambridge University Press.

Collier, Paul (1999). "On the Economic Consequences of Civil War." *Oxford Economic Papers*, 51, 168–183.

Coniglio, Nicola D. and Giovanni Pesce (2015). "Climate Variability and International Migration: An Empirical Analysis." *Environment and Development Economics*, 20, 434–468.

Conte, Bruno (2020). "Climate Change and Migration: The Case of Africa." Unpublished manuscript.

Conte, Bruno, Klaus Desmet, Dávid Krisztián Nagy, and Esteban Rossi-Hansberg (2021). "Local Sectoral Specialization in A Warming World." *Journal of Economic Geography*, 21, 493–530.

Costalli, Stefano, Luigi Moretti, and Costantino Pischedda (2017). "The Economic Costs of Civil War: Synthetic Counterfactual Evidence and the Effects of Ethnic Fractionalization." *Journal of Peace Research*, 54, 80–98.

Costinot, Arnaud, Dave Donaldson, and Cory Smith (2016). "Evolving Comparative Advantage and the Impact of Climate Change in Agricultural Markets: Evidence from 1.7 Million Fields Around the World." *Journal of Political Economy*, 124, 205–248.

Cruz, Jose-Louis and Esteban Rossi-Hansberg (2021). "The Economic Geography of Global Warming." NBER Working Paper No. 28466.

Dallmann, Ingrid and Katrin Millock (2017). "Climate Variability and Inter-State Migration in India." *CESifo Economic Studies*, 63, 560–594.

Dao, Thu, Frédéric Docquier, Mathilde Maurel, and Pierre Schaus (2018). "Migration and Development: Dissecting the Anatomy of the Mobility Transition." *Journal of Development Economics*, 101, 88–101.

Dell, Melissa, Benjamin F. Jones, and Benjamin A. Olken (2014). "What Do We Learn from the Weather? The New Climate-Economy Literature." *Journal of Economic Literature*, 52, 740–98.

Delogu, Marco, Frédéric Docquier, and Joël Machado (2018). "Globalizing Labor and the World Economy: The Role of Human Capital." *Journal of Economic Growth*, 23, 223–258.

Desmet, Klaus, Robert E. Kopp, Scott A. Kulp, Dávid Krisztián Nagy, Michael Oppenheimer, Esteban Rossi-Hansberg, and Benjamin H. Strauss (2021). "Evaluating the Economic Cost of Coastal Flooding." *American Economic Journal: Macroeconomics*, 13, 444–86.

Desmet, Klaus, Dávid Krisztián Nagy, and Esteban Rossi-Hansberg (2018). "The Geography of Development." *Journal of Political Economy*, 126, 903–983.

Desmet, Klaus and Esteban Rossi-Hansberg (2015). "On the Spatial Economic Impact of Global Warming." *Journal of Urban Economics*, 88, 16–37.

Deuster, Christoph (2021). "Climate Change and Educational Attainment: The Role of Human Mobility." *The Journal of Development Studies*, 57, 1527–1548.

Dilley, M., R.S. Chen, U. Deichmann, A.L. Lerner-Lam, M. Arnold, J. Agwe, P. Buys, B. Lyon, O. Kjekstad, and G. Yetman (2005). *Natural Disaster Hotspots: A Global Risk Analysis*. World Bank Publications.

Drabo, Alassane and Linguère Mously Mbaye (2015). "Natural Disasters, Migration and Education: An Empirical Analysis in Developing Countries." *Environment and Development Economics*, 20, 767–796.

Feenstra, R.C., R. Inklaar, and M.P. Timmer (2015). "The Next Generation of the Penn World Table." *American Economic Review*, 105, 3150–3182.

Findley, Sally E. (1994). "Does Drought Increase Migration? A Study of Migration from Rural Mali During the 1983–1985 Drought." *International Migration Review*, 28, 539–553.

Gemenne, François (2011). "Why the Numbers don't Add up: A Review of Estimates and Predictions of People Displaced by Environmental Changes." *Global Environmental Change*, 21, S41–S49.

Gleditsch, Nils Petter (2012). "Whither the Weather? Climate Change and Conflict." *Journal of Peace Research*, 49, 3–9.

Gleditsch, Nils Petter, Peter Wallensteen, Mikael Eriksson, Margareta Sollenberg, and Håvard Strand (2002). "Armed Conflict 1946-2001: A New Dataset." *Journal of Peace Research*, 39, 615–637.

Gollin, Douglas, David Lagakos, and Michael E. Waugh (2014). "The Agricultural Productivity Gap." *The Quarterly Journal of Economics*, 129, 939–993.

Gouel, Christophe and David Laborde (2021). "The Crucial Role of Domestic and International Market-Mediated Adaptation to Climate change." *Journal of Environmental Economics and Management*, 106, 102408.

Gray, Clark L. and Valerie Mueller (2012). "Natural Disasters and Population Mobility in Bangladesh." *Proceedings of the National Academy of Sciences*, 109, 6000–6005.

Grecequet, Martina, Jack DeWaard, Jessica J. Hellmann, and Guy J. Abel (2017). "Climate Vulnerability and Human Migration in Global Perspective." *Sustainability*, 9, 720.

Guha-Sapir, D. (2009). "EM-DAT: The Emergency Events Database." Working paper, Centre for Research on the Epidemiology of Disasters.

Haasnoot, Marjolijn, Judy Lawrence, and Alexandre K. Magnan (2021). "Pathways to Coastal Retreat." *Science*, 372, 1287–1290.

Hauer, Mathew E., Elizabeth Fussell, Valerie Mueller, Maxine Burkett, Maia Call, Kali Abel, Robert McLeman, and David Wrathall (2020). "Sea-Level Rise and Human Migration." *Nature Reviews Earth & Environment*, 1, 28–39.

Heal, Geoffrey and Jisung Park (2016). "Reflections' Temperature Stress and the Direct Impact of Climate Change: A Review of An Emerging Literature." *Review of Environmental Economics and Policy*, 10, 347–362.

Helbling, Marc and Daniel Meierrieks (2021). "How Climate Change Leads to Emigration: Conditional and Long-Run Effects." *Review of Development Economics*, 25, 2323–2349.

Henderson, J. Vernon, Adam Storeygard, and Uwe Deichmann (2017). "Has Climate Change Driven Urbanization in Africa?" *Journal of Development Economics*, 124, 60–82.

Hoffmann, Roman, Anna Dimitrova, Raya Muttarak, Jesus Crespo Cuaresma, and Jonas Peisker (2020). "A Meta-Analysis of Country-Level Studies on Environmental Change and Migration." *Nature Climate Change*, 10, 904–912.

Horton, Radley M., Alex de Sherbinin, David Wrathall, and Michael Oppenheimer (2021). "Assessing Human Habitability and Migration." *Science*, 372, 1279–1283.
IHME (2020). "Mapping Disparities in Education Across Low-and Middle-Income Countries." *Nature*, 577, 235.
IPCC (2014). *Climate Change 2014: Impacts, Adaptation, and Vulnerability. Contribution of Working Group II to the Fifth Assessment Report of the Intergovernmental Panel on Climate Change*. Cambridge University Press.
IPCC (2021). *Climate Change 2021: The Physical Science Basis. Contribution of Working Group I to the Sixth Assessment Report of the Intergovernmental Panel on Climate Change*. Cambridge University Press.
Jackson, Luke P. and Svetlana Jevrejeva (2016). "A Probabilistic Approach to 21st Century Regional Sea-Level Projections using RCP and High-end Scenarios." *Global and Planetary Change*, 146, 179–189.
Jayachandran, Seema (2006). "Selling Labor Low: Wage Responses to Productivity Shocks in Developing Countries." *Journal of Political Economy*, 114, 538–575.
Jevrejeva, Svetlana, Luke P. Jackson, Riccardo E.M. Riva, Aslak Grinsted, and John C. Moore (2016). "Coastal Sea Level Rise with Warming above 2 deg. C." *Proceedings of the National Academy of Sciences*, 113, 13342–13347.
Kennan, John (2013). "Open Borders." *Review of Economic Dynamics*, 16, L1–L13.
Kjellstrom, T., N. Maıtre, C. Saget, M. Otto, and T. Karimova (2019). *Working on A Warmer Planet: The Effect of Heat Stress on Productivity and Decent Work*. International Labour Office.
Klein, Paul and Gustavo Ventura (2009). "Productivity Differences and the Dynamic Effects of Labor Movements." *Journal of Monetary Economics*, 56, 1059–1073.
Kubik, Zaneta and Mathilde Maurel (2016). "Weather Shocks, Agricultural Production and Migration: Evidence from Tanzania." *The Journal of Development Studies*, 52, 665–680.
Kummu, Matti, Maija Taka, and Joseph H.A. Guillaume (2018). "Gridded Global Datasets for Gross Domestic Product and Human Development Index over 1990–2015." *Scientific Data*, 5, 1–15.
Lloyd, Christopher T., Alessandro Sorichetta, and Andrew J. Tatem (2017). "High Resolution Global Gridded Data for Use in Population Studies." *Scientific Data*, 4, 1–17.
Lobell, David B. and Marshall B. Burke (2010). "On the Use of Statistical Models to Predict Crop Yield Responses to Climate Change." *Agricultural and Forest Meteorology*, 150, 1443–1452.
Lucas, Robert E. (2009). "Trade and the Diffusion of the Industrial Revolution." *American Economic Journal: Macroeconomics*, 1, 1–25.
McFadden, Daniel L. (1974). "Conditional Logit Analysis of Qualitative Choice Behavior." *Frontiers in Econometrics*, Chapter 2, 105–142.
McLeman, Robert (2019). "International Migration and Climate Adaptation in an Era of Hardening Borders." *Nature Climate Change*, 9(12), 911–918.
Marchiori, Luca, Jean-François Maystadt, and Ingmar Schumacher (2012). "The Impact of Weather Anomalies on Migration in Sub-Saharan Africa." *Journal of Environmental Economics and Management*, 63, 355–374.
Marchiori, Luca, Jean-François Maystadt, and Ingmar Schumacher (2017). "Is Environmentally Induced Income Variability a Driver of Human Migration?" *Migration and Development*, 6, 33–59.
Mendelsohn, Robert, William D. Nordhaus, and Daigee Shaw (1994). "The Impact of Global Warming on Agriculture: A Ricardian Analysis." *The American Economic Review*, 84, 753–771.
Millock, Katrin (2015). "Migration and Environment." *Annual Review of Resource Economics*, 7, 35–60.
Moss, R. H., P. M. Reed, A. Hadjimichael, and J. Rozenberg (2021). "Planned Relocation: Pluralistic and Integrated Science and Governance." *Science*, 372, 1276–1279.
Mueller, Valerie, Clark Gray, and Katrina Kosec (2014). "Heat Stress Increases Long-Term Human Migration in Rural Pakistan." *Nature Climate Change*, 4, 182.
Murdoch, James C. and Todd Sandler (2004). "Civil wars and Economic Growth: Spatial Dispersion." *American Journal of Political Science*, 48, 138–151.

Nath, Ishan B. (2020). "The Food Problem and the Aggregate Productivity Consequences of Climate Change." NBER Working Paper No. 27297.

Nieves, Jeremiah J., Alessandro Sorichetta, Catherine Linard, Maksym Bondarenko, Jessica E. Steele, Forrest R. Stevens, Andrea E. Gaughan, Alessandra Carioli, Donna J. Clarke Thomas Esch, et al. (2020). "Annually Modelling Built-Settlements between Remotely-Sensed Observations Using Relative Changes in Subnational Populations and Lights at Night." *Computers, Environment and Urban Systems*, 80, 101444.

Nordhaus, William D. and Joseph Boyer (2000). *Warming the World: Economic Models of Global Warming*. MIT Press.

Oppenheimer, Michael, Bruce Glavovic, Jochen Hinkel, Roderik van de Wal, Alexandre K Magnan, Amro Abd-Elgawad, Rongshuo Cai, Miguel Cifuentes-Jara, Robert M Deconto Tuhin Ghosh, et al. (2019). *Sea Level Rise and Implications for Low Lying Islands, Coasts and Communities*. Intergovernmental Panel on Climate Change.

Ottaviano, Gianmarco I. P. and Giovanni Peri (2012). "Rethinking the Effect of Immigration on Wages." *Journal of the European Economic Association*, 10, 152–197.

Peri, Giovanni and Akira Sasahara (2019). "The Impact of Global Warming on Rural-Urban Migrations: Evidence from Global Big Data." NBER Working Paper, No. 25728.

Piguet, Etienne (2010). "Linking Climate Change, Environmental Degradation, and Migration: A Methodological Overview." *Climate Change*, 1, 517–524.

Piguet, Etienne, Antoine Pécoud, and Paul De Guchteneire (2011). "Migration and Climate Change: An Overview." *Refugee Survey Quarterly*, 30, 1–23.

Restuccia, Diego and Guillaume Vandenbroucke (2013). "The Evolution of Education: A Macroeconomic Analysis." *International Economic Review*, 54, 915–936.

Rigaud, K. K., B. Jones, J. Bergmann, V. Clement, K. Ober, J. Schewe, S. Adamo, B. McCusker, S. Heuser, and A. Midgley (2018). *Groundswell: Preparing for Internal Climate Migration*. The World Bank Group.

Shayegh, Soheil (2017). "Outward Migration May Alter Population Dynamics and Income Inequality." *Nature Climate Change*, 7, 828.

Skaperdas, Stergios (2011). "The Costs of Organized Violence: A Review of the Evidence." *Economics of Governance*, 12, 1–23.

Sorichetta, Alessandro, Tom J. Bird, Nick W. Ruktanonchai, Elisabeth zu Erbach-Schoenberg, Carla Pezzulo, Natalia Tejedor, Ian C. Waldock, Jason D. Sadler, Andres J. Garcia Luigi Sedda, et al. (2016). "Mapping Internal Connectivity through Human Migration in Malaria Endemic Countries." *Scientific Data*, 3, 1–16.

Stocker, Thomas F., Dahe Qin, Gian-Kasper Plattner, Melinda Tignor, Simon K. Allen, Judith Boschung, Alexander Nauels, Yu Xia, Vincent Bex, and Pauline M. Midgley (eds.) (2013). *Climate Change 2013: The Physical Science Basis. Contribution of Working Group I to the Fifth Assessment Report of the Intergovernmental Panel on Climate Change*. Cambridge University Press.

Stott, Peter (2016). "How Climate Change Affects Extreme Weather Events." *Science*, 352, 1517–1518.

Thiede, Brian, Clark Gray, and Valerie Mueller (2016). "Climate Variability and Inter-Provincial Migration in South America, 1970–2011." *Global Environmental Change*, 41, 228–240.

Vollrath, Dietrich (2009). "How Important are Dual Economy Effects for Aggregate Productivity?" *Journal of Development Economics*, 88, 325–334.

Watson, Christopher S., Neil J. White, John A. Church, Matt A. King, Reed J. Burgette, and Benoit Legresy (2015). "Unabated Global Mean Sea-Level Rise over the Satellite Altimeter Era." *Nature Climate Change*, 5, 565–568.

Supplementary Data

Supplementary data are available at *JEEA* online.